SUPPORTING MATERIAL

Assessment of Franck-Condon Methods for Computing Vibrationally Broadened UV/vis Absorption Spectra of Flavin Derivatives: Riboflavin, Roseoflavin and 5-Thioflavin

*Bora Karasulu, Jan Philipp Götze, Walter Thiel**

Max-Planck-Institut für Kohlenforschung, Kaiser-Wilhelm-Platz 1, 45470, Mülheim an der Ruhr, Germany

Contents:

Part A. Comparison of Gaussian and Lorentzian Broadening

Part B. Assignment of Predicted Vibrational Modes to Experimentally Observed Fundamental Modes for LF/S_0 and LF/S_1

Part C. Explicit Treatment of Hydrogen Bonding by Micro-Solvation

Supporting Tables: Tables S1-S6

Supporting Figures: Figures S1-S26

Part A. Comparison of Gaussian and Lorentzian Broadening

Table SI-A1. HWHM [cm^{-1}] vs. average overlap of intensities (O) [relative units] of the Gaussian/Lorentzian convoluted spectra from stick spectra using scaled (factor of 0.981) and unscaled CAM-B3LYP frequencies. See text for definition of O values.

Scaled			**Unscaled**		
HWHM	**Gaussian**	**Lorentzian**	**HWHM**	**Gaussian**	**Lorentzian**
5	0.36138	0.68740	5	0.31728	0.64458
10	0.56237	0.76375	10	0.52029	0.73572
15	0.66035	0.80314	15	0.63437	0.78419
20	0.72284	0.82754	20	0.70115	0.81352
25	0.76543	0.84321	25	0.74734	0.83253
30	0.79567	0.85460	30	0.78135	0.84531
35	0.81510	0.86360	35	0.80427	0.85506
40	0.82857	0.87081	40	0.81972	0.86248
45	0.83827	0.87644	45	0.82885	0.86870
50	0.84615	0.88094	50	0.83624	0.87389
55	0.85262	0.88443	55	0.84304	0.87816
60	0.85777	0.88697	60	0.84898	0.88174
65	0.86120	0.88927	65	0.85368	0.88448
70	0.86337	0.89142	70	0.85673	0.88689
75	0.86499	0.89343	75	0.85924	0.88917
80	0.86654	0.89532	80	0.86140	0.89134
85	0.86807	0.89711	85	0.86336	0.89341
90	0.86957	0.89881	90	0.86506	0.89539
95	0.87105	0.90044	95	0.86669	0.89727
100	0.87250	0.90201	100	0.86824	0.89907
150	0.88543	0.91505	150	0.88155	0.91375
200	0.89677	0.92460	200	0.89378	0.92453
250	0.90713	0.93158	250	0.90539	0.93278
300	0.91664	0.93643	300	0.91612	0.93905
350	0.92522	0.93918	350	0.92583	0.94364
500	0.94141	0.93941	500	0.94680	0.94748
1000	0.94071	0.93825	1000	0.94852	0.94576
Average	**0.82434**	**0.87908**	**Average**	**0.81464**	**0.87259**
Std.dev.	**0.12461**	**0.05662**	**Std.dev.**	**0.13627**	**0.06697**

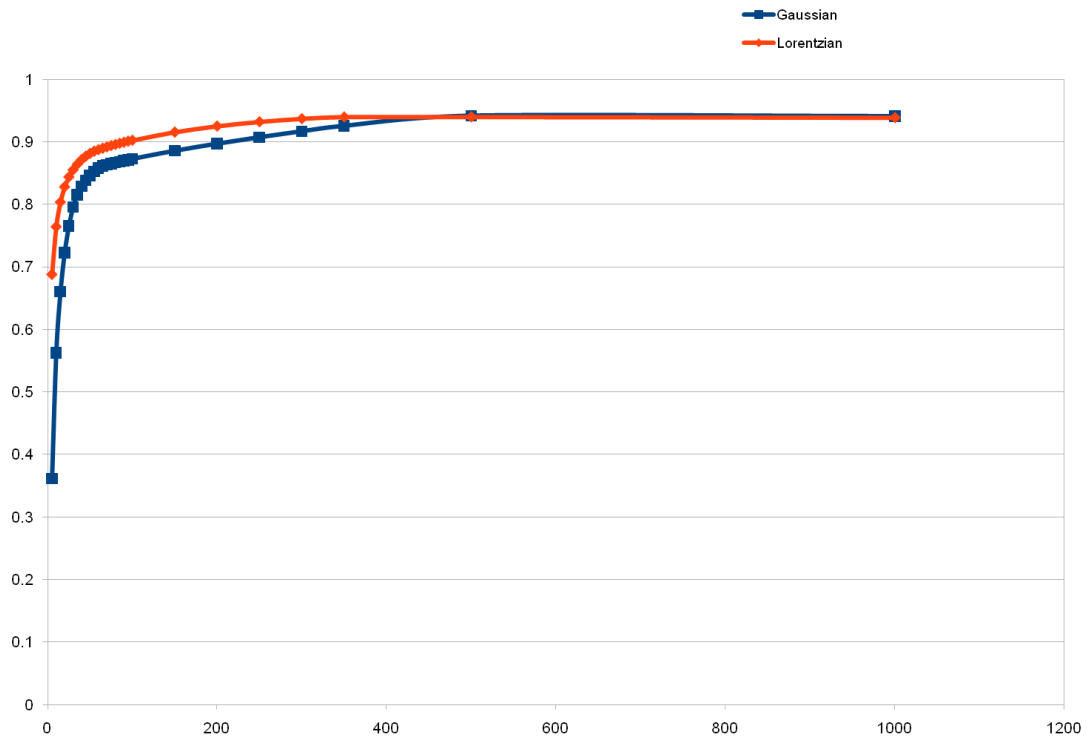

Figure SI-A1. Average overlap of intensities (O) vs. HWHM [cm^{-1}] with scaled CAM-B3LYP frequencies. See Table SI-A1 for corresponding numerical values.

As evident from Table SI-A1 and Figure SI-A1 (both for LF, first bright excited singlet state), Lorentzian broadening has a smaller standard deviation compared to Gaussian broadening for the O values computed with different HWHM values. This is as anticipated, since Lorentzians are associated with homogenous broadening (originating from natural life times), in contrast to the inhomogeneous broadening represented by Gaussians.[1–3] Therefore, only Lorentzian-broadened spectra are presented in the manuscript unless stated otherwise. Besides, use of higher HWHM values (larger than 100 cm^{-1}) always leads to more overlap (higher O value) between two given spectra (independent of the chosen method or broadening type). This is because the peak resolution is lowered by merging individual contributions from each vibrational level. Therefore, high HWHM values should not be used when two or

more computed spectra are compared to each other using the same reference spectrum.

Part B. Assignment of Predicted Vibrational Modes to Experimentally Observed Fundamental Modes of LF/S_0 and LF/S_1

Scaling of vibrational frequencies and ZPE corrections by a factor specific to the chosen computational method and basis set is a common practice (see ref [4] and references therein). Scaled harmonic vibrational frequencies of the LF/S_0 and LF/S_1 states at the CAS(8,8)/6-31G(d,p) level were shown to reproduce the experimental fundamental frequencies well.[5] Selected scaled fundamental frequencies from CAM-B3LYP/6-31G(d) and their CAS(8,8)/6-31G(d,p) counterparts are compared in Table SI-B1 with the experimental values measured in a He droplet. CAM-B3LYP performs well in this comparison. However, the success of the scaling procedure will generally be system-dependent. Therefore, we checked the effect of scaling the vibrational frequencies of LF/S_0 and LF/S_1 in more detail (see Table SI-B2 for the corresponding CAM-B3LYP results) and evaluated the quality of the generated spectra of LF/S_1 for all possible combinations of options (Table S1, visualized for one case in Figure S4). These tests show that scaling of frequencies may or may not slightly improve the resemblance between the computed and experimental spectra, but the changes are generally negligible (O values varying by less than 1%, Table S1). Therefore, in this study, we only present spectra resulting from unscaled frequencies (unless stated otherwise).

The measured peaks and their assignments to vibrational modes are compared in Table SI-B3 to their counterparts computed at the CAM-B3LYP level (visualized in Figure SI-B1). In the high-energy region ($\Delta\nu > 1000$ cm^{-1}), the deviation between

experimental and computed fundamental frequencies is quite pronounced, especially for the F8, F9, and F13 modes. The computed frequencies are blue-shifted relative to the fundamental frequencies by up to 30 cm^{-1}, which results in blue-shifted FC peak positions in the high-energy region.

Table SI-B1. Experimental fundamental vibrational wavenumbers (cm^{-1})[a] in the ground state (S_0) and first excited state (S_1), and their scaled counterparts computed at CASSCF(8,8)/6-31G(d,p)[a] and CAM-B3LYP/6-31G(d) levels of theory. For each set of computed vibrational frequencies, the average relative absolute error with respect to experimental frequencies and its standard deviation (excluding F12 and F13) are given. Scale factors of 0.933[a] and 0.981[b] are used for CAS(8,8) and CAM-B3LYP, respectively.

	He droplet[a]		**CAS(8,8)[a]**			**CAM-B3LYP**		
Name	**S_0**	**S_1**	**Label**	**S_0**	**S_1**	**Label**	**S_0**	**S_1**
F1	164	164	1a'	162	161	1a'	163	163
F2	280	274	3a'	293	284	2a'	278	274
F3	402	403	6a'	404	401	6a'	400	403
F4	443	440	7a'	441	442	7a'	440	441
F5	503	513	8a'	500	498	9a'	511	515
F6	596	593	11a'	602	599	11a'	599	598
F7	----	722	14a'	735	709	14a'	755	734
F8	988	978	18a'	986	983	19a'	1018	1005
F9	1167	1173	24a'	1165	1188	24a'	1165	1196
F10	1223	1205	25a'	1216	1212	25a'/26a'	1226	1222
F11	1342	1338	29a'	1326	1325	28a'/30a'	1309	1354
F12	1564	1507	Not given	--	--	38a'/41a'	1499	1508
F13	1600	1520	Not given	--	--	40a'/44a'	1517	1547
			Error:	0.011	0.014	**Error:**	0.011	0.010
			Std. dev.	0.013	0.011	**Std. dev.**	0.010	0.009

[a] taken from ref [5].
[b] taken from ref [4].

Table SI-B2. Unscaled ($\Delta\nu_U$) and scaled ($\Delta\nu_S$) ground-state (S_0) and excited-state (S_1) vibrational frequencies computed at the CAM-B3LYP/6-31G(d) level of theory. The fundamental modes are marked in bold.

Ground state (S_0)						Excited state (S_1)					
Symm	$\Delta\nu_U$	$\Delta\nu_S$	Symm	$\Delta\nu_U$	$\Delta\nu_S$	Symm	$\Delta\nu_U$	$\Delta\nu_S$	Symm	$\Delta\nu_U$	$\Delta\nu_S$
1a'	166	162.8	1a"	44	43.2	**1a'**	**166**	**162.8**	1a"	43	42.2
2a'	283	277.6	2a"	64	62.8	**2a'**	**280**	**274.7**	2a"	49	48.1
3a'	300	294.3	3a"	101	99.1	3a'	299	293.3	3a"	97	95.2
4a'	329	322.7	4a"	126	123.6	4a'	325	318.8	4a"	121	118.7
5a'	359	352.2	5a"	140	137.3	5a'	362	355.1	5a"	132	129.5
6a'	**408**	**400.2**	6a"	152	149.1	**6a'**	**411**	**403.2**	6a"	158	155.0
7a'	**448**	**439.5**	7a"	175	171.7	**7a'**	**449**	**440.5**	7a"	164	160.9
8a'	509	499.3	8a"	192	188.3	8a'	498	488.5	8a"	192	188.4
9a'	**521**	**511.1**	9a"	209	205.0	**9a'**	**525**	**515.0**	9a"	220	215.8
10a'	551	540.5	10a"	252	247.2	10a'	551	540.5	10a"	240	235.4
11a'	**611**	**599.4**	11a"	338	331.6	**11a'**	**610**	**598.4**	11a"	323	316.9
12a'	648	635.7	12a"	382	374.7	12a'	643	630.8	12a"	335	328.6
13a'	683	670.0	13a"	463	454.2	13a'	673	660.2	13a"	415	407.1
14a'	**770**	**755.4**	14a"	526	516.0	**14a'**	**748**	**733.8**	14a"	480	470.9
15a'	801	785.8	15a"	641	628.8	15a'	788	773.0	15a"	615	603.3
16a'	847	830.9	16a"	676	663.1	16a'	839	823.1	16a"	645	632.7
17a'	887	870.1	17a"	728	714.2	17a'	883	866.2	17a"	678	665.1
18a'	**1022**	**1002.6**	18a"	771	756.3	**18a'**	**1013**	**993.8**	18a"	730	716.1
19a'	1038	1018.3	19a"	778	763.2	19a'	1024	1004.5	19a"	740	725.9
20a'	1055	1035.0	20a"	813	797.5	20a'	1040	1020.2	20a"	761	746.5
21a'	1059	1038.9	21a"	885	868.2	21a'	1055	1035.0	21a"	874	857.4
22a'	1120	1098.7	22a"	940	922.1	22a'	1107	1086.0	22a"	911	893.7
23a'	1188	1165.4	23a"	1073	1052.6	23a'	1182	1159.5	23a"	1062	1041.8
24a'	**1214**	**1190.9**	24a"	1096	1075.2	**24a'**	**1219**	**1195.8**	24a"	1083	1062.4
25a'	1250	1226.3	25a"	1172	1149.7	25a'	1240	1216.4	25a"	1166	1143.8
26a'	**1273**	**1248.8**	26a"	1513	1484.2	**26a'**	**1246**	**1222.3**	26a"	1508	1479.3
27a'	1313	1288.1	27a"	1529	1499.9	27a'	1293	1268.4	27a"	1524	1495.0
28a'	**1334**	**1308.7**	28a"	1545	1515.6	28a'	1313	1288.1	28a"	1535	1505.8
29a'	1359	1333.2	29a"	3128	3068.5	29a'	1350	1324.4	29a"	3119	3059.7
30a'	1396	1369.5	30a"	3134	3074.4	**30a'**	**1381**	**1354.8**	30a"	3125	3065.6
31a'	1412	1385.2	31a"	3168	3107.8	31a'	1400	1373.4	31a"	3158	3098.0
32a'	1433	1405.8				32a'	1422	1395.0			
33a'	1448	1420.5				33a'	1431	1403.8			
34a'	1451	1423.4				34a'	1449	1421.5			
35a'	1464	1436.2				35a'	1452	1424.4			
36a'	1479	1450.9				36a'	1461	1433.2			
37a'	1500	1471.5				37a'	1467	1439.1			
38a'	**1528**	**1499.0**				38a'	1485	1456.8			
39a'	1533	1503.9				39a'	1510	1481.3			
40a'	**1546**	**1516.6**				40a'	1527	1498.0			
41a'	1572	1542.1				**41a'**	**1537**	**1507.8**			
42a'	1636	1604.9				42a'	1564	1534.3			

43a'	1649	1617.7				43a'	1566	1536.2			
44a'	1696	1663.8				**44a'**	**1577**	**1547.0**			
45a'	1730	1697.1				45a'	1674	1642.2			
46a'	1859	1823.7				46a'	1803	1768.7			
47a'	1868	1832.5				47a'	1824	1789.3			
48a'	3073	3014.6				48a'	3067	3008.7			
49a'	3077	3018.5				49a'	3072	3013.6			
50a'	3099	3040.1				50a'	3092	3033.3			
51a'	3168	3107.8				51a'	3162	3101.9			
52a'	3169	3108.8				52a'	3176	3115.7			
53a'	3239	3177.5				53a'	3245	3183.3			
54a'	3240	3178.4				54a'	3246	3184.3			
55a'	3255	3193.2				55a'	3252	3190.2			
56a'	3629	3560.0				56a'	3636	3566.9			

Table SI-B3. Franck-Condon pattern of the excitation spectrum of LF/S_1 in the gas phase. The measured vibrational peak intensities are compared to the FC factors from the TI/IMDHO-FA+AFC model, computed using the vibrational modes at the CAM-B3LYP level. Relative shifts ($\Delta\nu$, cm^{-1}) and relative intensities (I, relative units) are given for each vibrational progression. For each peak, the relative absolute error of the computed relative shifts and intensities with respect to their measured counterparts are also given. Some peaks have two possible assignments. In these cases, we present the most plausible assignment in bold based on the relative intensity and relative shift of the corresponding peak. Large deviations from the experiment are indicated in red.

Experiment[a]				CAM-B3LYP6-31G(d)				
Position (cm^{-1})	**Content**	**Δv**	**I**	**Content**	**Δv**	**I**	**Relative error (Δv)**	**Relative error (I)**
21511	0-0	0	1.00	0-0	0	1.00	N/A	0.000
21675	F1	164	0.59	F1	163	0.83	0.006	0.415
21785	F2	274	0.11	F2	274	0.07	0.000	0.394
				F2*	294	0.06	N/A	N/A
21838	2F1	327	0.29	2F1	326	0.35	0.003	0.196
21914	F3	403	0.15	F3	403	0.08	0.000	0.451
21951	F4	440	0.15	F4	441	0.03	0.002	0.822
22005	3F1	494	0.11	3F1	489	0.10	0.010	0.131
22024	F5	513	0.22	F5	515	0.24	0.004	0.075
22078	F1+F3	567	0.11	F1+F3	566	0.07	0.002	0.366
22104	F6	593	0.11	F6	598	0.04	0.008	0.627
22192	F1+F5	681	0.22	F1+F5	678	0.20	0.004	0.102

22233	F7	722	0.15	F7	734	0.06	0.017	0.582
22268	F1+F6	757	0.11	F1+F6	761	0.03	0.005	0.683
22296	F2+F5	785	0.08	F2+F5	789	0.02	0.005	0.785
22318	2F3	807	0.08	2F3	807	0.00	0.000	0.956
				F7*	823	0.04	N/A	N/A
22355	2F1+F5	844	0.11	2F1+F5	841	0.08	0.004	0.254
22400	F1+F7	889	0.08	F1+F7	897	0.05	0.009	0.334
	F3+F5			F3+F5	**918**	**0.02**	**0.001**	**0.478**
22430	OR	919	0.04	OR	OR	OR	OR	OR
	2F1+F6			2F1+F6	1020	0.00	0.110	0.996
22489	F8	978	0.15	F8	1005	0.03	0.028	0.827
22540	2F5	1029	0.11	2F5	1030	0.03	0.001	0.742
22562	2F1+F7	1051	0.04	2F1+F7	1060	0.02	0.009	0.436
22593	F1+F3+F5	1082	0.04	F1+F3+F5	1081	0.02	0.001	0.558
22615	F5+F6	1104	0.04	F5+F6	1276	0.01	0.156	0.818
22653	F1+F8	1142	0.11	F1+F8	1175	0.03	0.022	0.806
22684	F9	1173	0.15	F9	1196	0.03	0.019	0.827
22716	F10	1205	0.15	F10	1222	0.03	0.014	0.767
22748	F5+F7	1237	0.15	F5+F7	1249	0.01	0.010	0.905
				F10*	1268	0.07	N/A	N/A
22849	F11	1338	0.29	F11	1355	0.13	0.013	0.543
22878	F1+F10	1367	0.22	F1+F10	1385	0.03	0.013	0.871
22914	F1+F5+F7	1403	0.11	F1+F5+F7	1412	0.01	0.006	0.890
				F11*	1404	0.10	N/A	N/A
				F11**	1425	0.47	N/A	N/A
				F11***	1439	0.06	N/A	N/A
22994	F1+F6+F7	1483	0.15	F1+F6+F7	1495	0.00	0.008	0.983
	F12			F12	1508	0.00	0.001	0.997
23018	OR	1507	0.22	OR	OR	OR	OR	OR
	F1+F11			F1+F11	**1518**	**0.11**	**0.007**	**0.485**
23031	F13	1520	0.18	F13	1547	0.14	0.018	0.219
23045	2F1+F10	1534	0.22	2F1+F10	1542	0.01	0.009	0.948
				F1+F11**	1587	0.38	N/A	N/A
23084	F3+F9	1573	0.11	F3+F9	1599	0.00	0.017	0.986
	F1+F12			F1+F12	**1670**	**0.00**	**0.001**	0.998
23183	OR	1672	0.18	OR	OR	OR	OR	OR
	2F1+F11			2F1+F11	1777	0.00	0.063	0.997
23214	F7+F8	1703	0.15	F7+F8	1734	0.00	0.018	0.988
				2F1+F11**	1750	0.16	N/A	N/A
23251	F1+F3+F9	1740	0.11	F1+F3+F9	1762	0.00	0.013	0.989
23365	F1+F5+F9	1854	0.11	F1+F5+F9	1873	0.01	0.010	0.954

[a] taken from ref. [5].

*The CAM-B3LYP calculations predict additional C1 overtones with high intensities that have not been assigned in Ref [5] but are included here (marked with an asterisk).

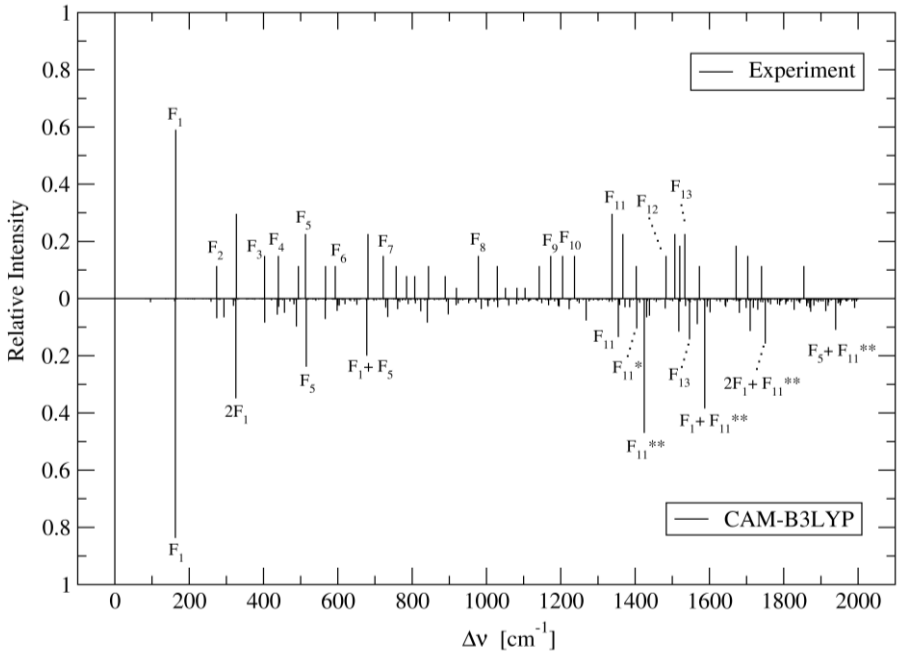

Figure SI-B1. Comparison of the experimental progression peaks (taken from ref [5]) to the FC factors computed using the scaled vibrational frequencies at the CAM-B3LYP/6-31G(d) level. Detailed assignments and characterizations of the progression peaks are given Table SI-B2.

Part C. Explicit Treatment of Hydrogen Bonding by Micro-Solvation

In order to check the effect of explicit H-bond networks on the absorption spectra, we created three different micro-hydration models of RoLF as introduced for LF in Ref [6,7] (see Figure SI-C1) and combined them with implicit solvent models (COSMO, CPCM). We placed several water molecules in close proximity of the H-bond acceptors located in the hydrophilic region of the isoalloxazine moiety as well as close to the DMA group located in the hydrophobic region. These models are just a small sample from the whole ensemble of different possible interaction schemes of water molecules with RoLF, acting as indicator for possible effects.

As evident from the DFT/MRCI results collected in Table SI-C1, consideration of explicit water molecules (model B, C, and D) affects the vertical transition energies

and oscillator strengths to different extents for different electronic states. The effects are in line with rearrangements of the electronic density distribution caused by the water molecules. What is striking here is that the oscillator strength of the dark S_2 state (of $n\pi^*$ character) is increased when a water molecule is placed juxtaposed to the DMA group (model D). Therefore, the S_2 state will likely contribute to the absorption spectrum of RoLF, a feature not seen from the implicit solvation models. Considering the energy separation between the S_1 and S_2 states and the medium oscillator strength in the micro-hydration scheme, the missing second band in the predicted spectra (main article, see Figure 8) can be attributed to missing H-bonds.

To further elaborate on this, we compare the VFC spectra using TD/IMDHO-FA model without (model A) and with micro-solvation (model D) with the experimental spectrum in Figure SI-C2. The water network including the H-bond to the DMA group lowers the intensity of the band formed by the $S_0 \rightarrow S_1$ transition, which leads to better qualitative agreement with the experiment (Figure SI-C2). It also assigns more intensity to the second band attributed to the $S_0 \rightarrow S_2$ transition, such that this band is almost of equal height as in the experimental spectrum. One aspect to notice here is the blue shift of the second band with respect to the experiment, which may be related to the use of a small basis set (SVP) that is insufficient to predict the vertical transition energies accurately. Another reason for the blue-shift may be as follows. The chosen micro-solvation model is rather small (containing only a few water molecules), and the more extended real water network may have more impact, e.g., by further stabilizing the "CT-like" S_2 state and thus shifting the corresponding band to higher wavelength.

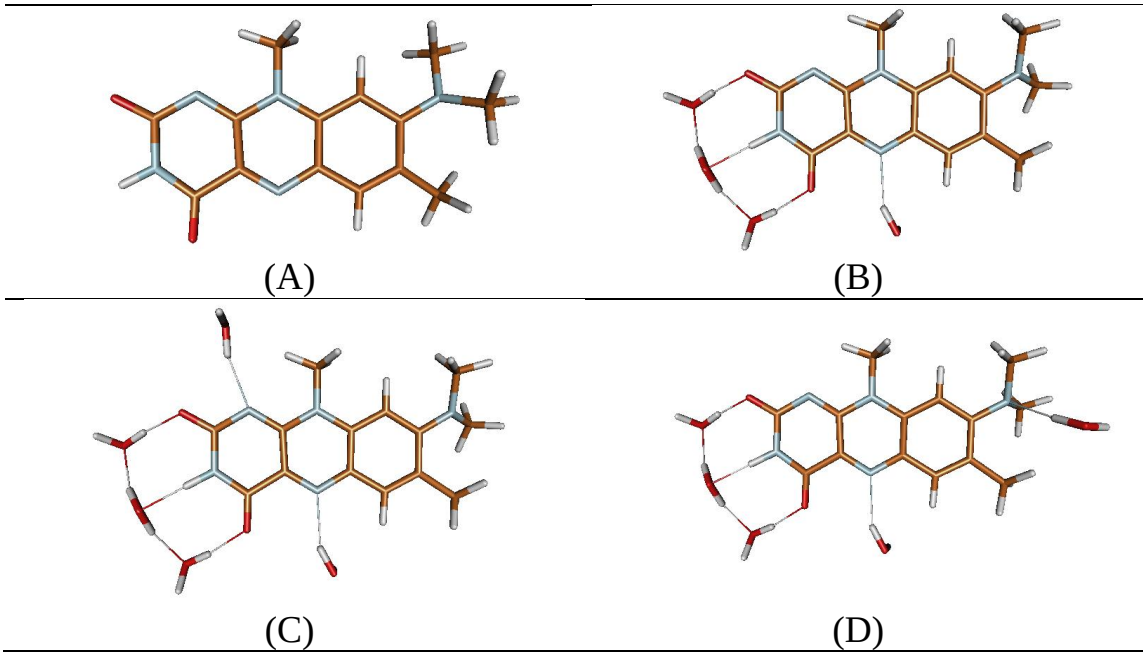

Figure SI-C1. Four different models used to investigate the effects of explicit solvation for RoLF: (A) without micro-solvation, (B) 4-water model (H-bonds to O2, N3, O4, and N5), (C) 5-water model (one extra water molecule H-bonded to N1), (D) 5-water model (one extra water molecule H-bonded to the DMA group). Geometries shown here are the ground-state minima obtained at the CAM-B3LYP/6-31G(d) level.

Table SI-C1. Vertical transition energies (E_{vert}), oscillator strengths (f), and dipole moments (μ) for relevant singlet excited states of the model systems depicted in Figure SI-C1

	Model A (KS orbitals from BHLYP/TZVP used for DFT/MRCI)				Model A (KS orbitals from BHLYP/SVP used for DFT/MRCI)			
State	**E_{vert} [eV]**	**E_{vert} [nm]**	**f**	**μ [Debye]**	**E_{vert} [eV]**	**E_{vert} [nm]**	**f**	**μ [Debye]**
S_0	---	---	---	17.28	---	---	---	16.29
S_1	2.76	449	0.70305	21.98	2.80	442	**0.69950**	20.83
S_2	3.16	393	0.00975	22.9	3.23	384	**0.01518**	22.33
S_3	3.57	347	0.00272	15.74	3.51	353	0.00338	14.62
S_4	3.89	319	0.00010	9.74	3.75	331	0.00011	8.53
S_5	4.07	305	0.01510	21.59	4.14	300	0.01422	20.46
S_6	4.41	281	0.03409	17.61	4.40	282	0.00155	10.25
S_7	4.56	272	0.11685	17.03	4.41	281	0.00036	8.37
S_8	4.62	268	0.00136	9.35	4.61	269	0.15729	19.67
S_9	4.80	259	0.34395	15.45	4.78	259	0.00405	12.47
S_{10}	4.89	254	0.00066	13.23	4.83	257	0.39111	16.21
S_{11}	4.95	250	0.13351	21.57	5.05	246	0.09996	20.93
S_{12}	5.21	238	0.79191	22.27	5.29	234	0.78394	21.32

Table SI-C1 continued.

	Model B (KS orbitals from BHLYP/SVP used for DFT/MRCI)				Model C (KS orbitals from BHLYP/SVP used for DFT/MRCI)				Model D (KS orbitals from BHLYP/SVP used for DFT/MRCI)			
State	**E_{vert} [eV]**	**E_{vert} [nm]**	**f**	**μ [Debye]**	**E_{vert} [eV]**	**E_{vert} [nm]**	**f**	**μ [Debye]**	**E_{vert} [eV]**	**E_{vert} [nm]**	**f**	**μ [Debye]**
S_0	---	---	---	19.74	---	---	---	19.46	---	---	---	16.9
S_1	2.68	463	0.77813	24.85	2.67	465	0.78353	24.81	2.86	433	**0.53141**	18.87
S_2	3.12	397	0.00466	23.55	3.15	394	0.01033	22.41	3.29	377	**0.15876**	26.00
S_3	3.55	349	0.00283	17.83	3.60	345	0.00301	17.93	3.46	358	0.00358	15.24
S_4	3.89	319	0.00015	11.27	3.89	319	0.00015	11.18	3.80	326	0.00019	9.30
S_5	4.04	307	0.01425	23.34	4.04	307	0.01689	22.94	4.09	303	0.00810	21.39
S_6	4.35	285	0.01763	18.27	4.34	286	0.04552	20.38	4.34	285	0.00780	10.84
S_7	4.50	275	0.04765	13.90	4.50	276	0.03785	11.71	4.39	282	0.01124	10.65
S_8	4.53	273	0.11919	16.48	4.54	273	0.11585	14.63	4.59	270	0.00094	14.17
S_9	4.67	265	0.00139	15.80	4.80	258	0.21375	19.02	4.76	260	0.16059	20.40
S_{10}	4.80	258	0.26961	19.43	4.83	257	0.00712	14.60	4.83	257	0.50411	17.55
S_{11}	4.99	248	0.15303	23.88	4.99	248	0.14377	23.33	5.03	246	0.05806	22.55
S_{12}	5.18	239	0.85233	23.95	5.17	240	0.88860	23.10	5.42	229	0.79918	22.07

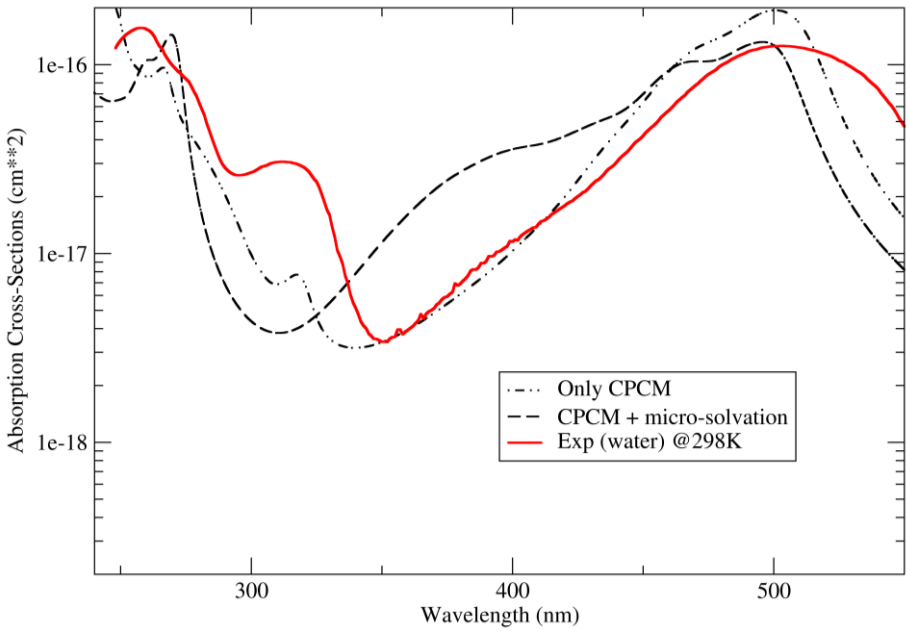

Figure SI-C2. MRCI-corrected TD/IMDHO-FA VFC spectra of model A and model D obtained at the CAM-B3LYP/6-31G(d) level in comparison to the experimental spectrum. The Kohn-Sham orbitals used in the DFT/MRCI calculations were obtained for both models at the BHLYP/SVP level.

Supporting Tables

Table S1. Average O values and standard deviations (spectral yield, C, in parentheses) for experimental and computed VFC and AFC (at eclipsed and staggered minima) spectra at different levels of theory using unscaled and scaled vibrational frequencies. Nimag: Number of imaginary modes, Rect/Curv: rectilinear/curvilinear representation.

	BP86		**B3LYP**		**CAM-B3LYP**		**ωB97xD**	
	Rect	**Curv**	**Rect**	**Curv**	**Rect**	**Curv**	**Rect**	**Curv**
VFC								
N_{imag}	2		2		2		2	
Unscaled	0.632 ± 0.026 (0.632)	0.632 ± 0.026 (0.632)	0.752 ± 0.038 (0.835)	0.752 ± 0.038 (0.835)	0.868 ± 0.029 (0.853)	0.866 ± 0.058 (0.854)	0.860 ± 0.058 (0.856)	0.860 ± 0.060 (0.856)
AFC - Eclipsed conformation								
N_{imag}	1		1		0		0	
Unscaled	0.706 ± 0.034 (0.816)	0.706 ± 0.034 (0.816)	0.782 ± 0.036 (0.860)	0.778 ± 0.036 (0.857)	0.866 ± 0.066 (0.947)	0. 866± 0.066 (0.947)	0.864 ± 0.066 (0.925)	0.864 ± 0.066 (0.926)
Scaled[a]	0.710 ± 0.034 (0.816)	0.706 ± 0.034 (0.816)	0.778 ± 0.034 (0.860)	0.774 ± 0.034 (0.857)	0.874 ± 0.056 (0.947)	0.874± 0.056 (0.947)	0.870 ± 0.054 (0.925)	0.870 ± 0.056 (0.926)
AFC - Staggered conformation								
N_{imag}	2		1		1		1	
Unscaled	0.156 ± 0.020 (0.000)	0.108 ± 0.030 (0.016)	**No spectrum**	0.154 ± 0.032 (0.055)	0.156 ± 0.020 (0.000)	0.202 ± 0.024 (0.170)	0.092 ± 0.006 (0.000)	0.140 ± 0.030 (0.091)
Scaled[a]	0.156 ± 0.020 (0.000)	0.106 ± 0.032 (0.016)	**No spectrum**	0.154 ± 0.032 (0.055)	0.156 ± 0.020 (0.000)	0.198 ± 0.024 (0.170)	0.088 ± 0.006 (0.000)	0.138 ± 0.030 (0.091)

[a] Scale factors of 0.991, 0.981, 1.005, and 0.980 were used for B3LYP, CAM-B3LYP, BP86, and ωB97xD, respectively.[4]

Table S2. Effect of the chosen basis set on the CAM-B3LYP results. See Table 1 for the definition of the abbreviations.

	AFC - Eclipsed conformation				
	STO-3G[a]	**6-31G(d)**	**6-31++G(d,p)**	**6-311++G(d,p)**	**TZVP**
$RMSD^{Cart}$	0.04444	0.04208	0.04084	0.04122	0.04047
$RMSD^{Bonds}$	0.02791	0.01956	0.01911	0.01962	0.01991
$RMSD^{Ang}$	1.43405	1.26380	1.23612	1.24655	1.24073
$RMSD^{Dihed}$	0.10735	0.13193	0.13461	0.13965	0.13864
C_{rect}	0.783	0.947	0.940	0.933	0.913
C_{curv}	0.780	0.947	0.941	0.933	0.912
O_{rect}	0.734±0.032	0.866± 0.066	0. 878 ± 0.066	0.880 ± 0.064	0.880 ± 0.066
O_{curv}	0.724±0.032	0.866± 0.066	0.878 ± 0.066	0.880 ± 0.064	0.880 ± 0.066

[a]Only for STO-3G: the optimized geometry is a saddle point with one imaginary-frequency mode, which was ignored as in the VFC approach.

Table S3. List of the bright states of **LF** at the respective ground-state minimum in vacuum, benzene, and water: oscillator strengths (f) and vertical excitation energies (E_{vert} in eV) computed at the TD-CAM-B3LYP, B3LYP and DFT/MRCI levels of theory, along with the correction energies for the DFT/MRCI correction scheme.

Gas Phase							
CAM-B3LYP			**DFT/MRCI**			**Correction**	**AFC min.**
State	**f**	**E_{vert}**	**State**	**f**	**E_{vert}**	**ΔE_{vert}**	**available?**
S_1	0.2904	3.46	S_1	0.3187	2.99	0.47	yes
S_4	0.1269	4.41	S_4	0.2064	3.87	0.54	yes
S_8	0.6752	5.32	S_9	0.4133	4.80	0.52	yes
S_9	0.1067	5.41	S_{10}	0.4126	4.93	0.48	no
Benzene							
CAM-B3LYP			**DFT/MRCI**			**Correction**	**AFC min.**
State	**f**	**E_{vert}**	**State**	**f**	**E_{vert}**	**ΔE_{vert}**	**available?**
S_1	0.4169	3.34	S_1	0.3191	2.96	0.38	yes
S_4	0.2094	4.25	S_4	0.2255	3.78	0.47	no
S_8	0.8270	5.23	S_9	0.5107	4.81	0.42	no
S_9	0.0276	5.36	S_{10}	0.3126	4.94	0.38	no
Water							
CAM-B3LYP			**DFT/MRCI**			**Correction**	**AFC min.**
State	**f**	**E_{vert}**	**State**	**f**	**E_{vert}**	**ΔE_{vert}**	**available?**
S_1	0.3809	3.33	S_1	0.2992	2.93	0.40	yes
S_3	0.2153	4.11	S_3	0.2641	3.60	0.51	yes
S_5	0.1946	5.00	S_6	0.0185	4.56	0.44	no
S_8	0.5524	5.30	S_8	0.6079	4.83	0.53	yes
S_{10}	0.1245	5.78	S_{10}	0.2416	4.98	0.80	yes
Benzene							
B3LYP			**DFT/MRCI**			**Correction**	
State	**f**	**E_{vert}**	**State**	**f**	**E_{vert}**	**ΔE_{vert}**	
S_1	0.2755	2.95	S_1	0.3149	2.88	0.07	
S_4	0.2253	3.72	S_4	0.2268	3.69	0.03	
S_9	0.7645	4.80	S_9	0.5234	4.74	0.06	
Water							
B3LYP			**DFT/MRCI**			**Correction**	
State	**f**	**E_{vert}**	**State**	**f**	**E_{vert}**	**ΔE_{vert}**	
S_1	0.2325	2.94	S_1	0.29294	2.85	0.09	
S_4	0.2388	3.61	S_3	0.26632	3.52	0.09	
S_9	0.7668	4.83	S_9	0.63177	4.76	0.07	

DFT/MRCI calculations were done at the respective GS minimum of the listed density functional. According to the DFT/MRCI results, the third absorption band has contribution from a single excitation (S_9) at the B3LYP minimum geometry and from two excitation states (S_8 and S_9) at the CAM-B3LYP minimum geometry. AFC

spectra were not calculated for B3LYP, thus the column "AFC min available" is missing in this case.

Table S4. List of the bright states of **RoLF** at the respective ground-state minimum in vacuum and water: oscillator strengths (f) and vertical excitation energies (E_{ver} in eV_t) computed at the TD-CAM-B3LYP, ωB97xD, B3LYP, and DFT/MRCI levels of theory, along with the correction energy for the DFT/MRCI correction scheme.

Gas phase							
CAM-B3LYP			**DFT/MRCI**			**Correction**	**AFC min.**
State	**f**	**E_{vert}**	**State**	**f**	**E_{vert}**	**ΔE_{vert}**	**available?**
S_1	0.4601	3.39	S_1	0.4986	2.92	0.47	yes
S_4	0.0920	4.10	S_4	0.1457	3.52	0.58	no
S_9	0.4215	5.29	S_{10}	0.5722	4.78	0.51	no
Benzene							
CAM-B3LYP			**DFT/MRCI**			**Correction**	**AFC min.**
State	**f**	**E_{vert}**	**State**	**f**	**E_{vert}**	**ΔE_{vert}**	**available?**
S_1	0.6802	3.22	S_1	0.5673	2.88	0.34	yes
S_3	0.0824	3.91	S_3	0.1026	3.39	0.52	no
S_8	0.2894	5.19	S_8	0.1194	4.65	0.54	yes
S_{10}	0.4602	5.35	S_{10}	0.4732	4.77	0.58	no
Water							
CAM-B3LYP			**DFT/MRCI**			**Correction**	**AFC min.**
State	**f**	**E_{vert}**	**State**	**f**	**E_{vert}**	**ΔE_{vert}**	**available?**
S_1	0.7209	3.16	S_1	0.7030	2.76	0.40	yes
S_2	0.0363	3.74	S_2	0.0097	3.16	0.58	no
S_5	0.0105	4.75	S_5	0.0152	4.07	0.68	no
S_6	0.1794	4.94	S_6	0.0341	4.41	0.53	yes
S_8	0.2141	5.21	S_{11}	0.1334	4.95	0.26	no
S_{10}	0.4929	5.41	S_7	0.1167	4.56	0.85	yes
S_{11}	0.1470	5.71	S_9	0.3441	4.80	0.91	no
S_{12}	0.3765	5.96	S_{12}	0.7921	5.21	0.75	no
Water							
wB97xD			**DFT/MRCI**			**Correction**	
State	**f**	**E_{vert}**	**State**	**f**	**E_{vert}**	**ΔE_{vert}**	
S_1	0.7265	3.16	S_1	0.7128	2.74	0.42	
S_6	0.1641	4.94	S_6	0.0482	4.39	0.39	
S_8	0.2432	5.23	S_{12}	0.7556	5.19	0.04	
S_{10}	0.4710	5.44	S_7	0.1036	4.55	0.89	
S_{11}	0.1619	5.71	S_9	0.2924	4.78	0.93	
S_{12}	0.3133	6.00	S_{11}	0.2090	4.94	1.06	
Water							
B3LYP			**DFT/MRCI**			**Correction**	
State	**f**	**E_{vert}**	**State**	**f**	**E_{vert}**	**ΔE_{vert}**	

S_1	0.6433	2.81	S_1	0.7361	2.66	0.15
S_8	0.1389	4.43	S_7	0.1136	4.48	-0.05
S_{10}	0.4818	4.90	S_9	0.2521	4.72	0.18
S_{11}	0.2799	5.05	S_{11}	0.2552	4.89	0.16
S_{12}	0.3968	5.16	S_{12}	0.6775	5.10	0.06

DFT/MRCI calculations were done at the respective GS minimum of the listed density functional. Matching of states between CAM-B3LYP and MRCI was done based on the dominant excitations; therefore, the MRCI states are not always in increasing order. AFC spectra were not calculated for ωB97xD and B3LYP, thus the column "AFC min available" is missing in this case.

Table S5. List of the bright states of **5TLF-Neutral form** at the respective ground state minimum in vacuum and water: oscillator strengths (f) and vertical excitation energies (E_{vert} in eV) computed at the TD-CAM-B3LYP, B3LYP, and DFT/MRCI levels of theory, along with the correction energy for the DFT/MRCI correction scheme.

Water						
CAM-B3LYP			**DFT/MRCI**			**Correction**
State	**f**	**E_{vert}**	**State**	**f**	**E_{vert}**	**ΔE_{vert}**
S_1	0.0593	3.89	S_1	0.0397	3.60	0.29
S_2	0.2650	4.75	S_2	0.0441	4.18	0.57
S_3	0.1117	4.96	S_3	0.1714	4.48	0.48
S_4	0.2566	5.45	S_4	0.0781	5.02	0.43
S_5	0.1441	5.57	S_6	0.1288	5.18	0.39
S_6	0.3589	5.64	S_5	0.1186	5.08	0.56
S_7	0.1138	5.82	S_8	0.2118	5.31	0.51
S_8	0.4018	5.88	S_7	0.3208	5.24	0.64
S_9	0.2878	6.24	S_9	0.1376	5.62	0.62

Water						
B3LYP			**DFT/MRCI**			**Correction**
State	**f**	**E_{vert}**	**State**	**f**	**E_{vert}**	**ΔE_{vert}**
S_1	0.0262	3.47	S_1	0.0428	3.54	-0.07
S_2	0.1077	4.25	S_3	0.1672	4.41	-0.16
S_3	0.0575	4.46	S_2	0.0407	4.12	0.34
S_4	0.0162	4.86	S_4	0.0843	4.97	-0.11

S_5	0.2760	4.95	S_5	0.1169	5.01	-0.06
S_6	0.0570	5.10	S_6	0.0119	5.12	-0.02
S_7	0.0424	5.14	S_7	0.3328	5.17	-0.03
S_8	0.1347	5.25	S_8	0.2122	5.24	0.01
S_9	0.0755	5.57	S_9	0.1303	5.55	0.02
S_{10}	0.0234	5.86	S_{10}	0.0313	5.81	0.05

Table S6. List of the bright states of **5TLF-Anionic form** at the respective ground state minimum in vacuum and water: oscillator strengths (f) and vertical excitation energies (E_{vert} in eV) computed at the TD-CAM-B3LYP, B3LYP and DFT/MRCI levels of theory, along with the correction energy for the DFT/MRCI correction scheme.

Water						
CAM-B3LYP			**DFT/MRCI**			**Correction**
State	**f**	**E_{vert}**	**State**	**f**	**E_{vert}**	**ΔE_{vert}**
S_1	0.0084	4.02	S_1	0.0150	3.72	0.30
S_2	0.2162	4.58	S_2	0.0717	4.08	0.50
S_3	0.1804	4.99	S_3	0.1376	4.57	0.42
S_4	0.5650	5.18	S_5	0.3314	4.89	0.29
S_5	0.1632	5.38	S_4	0.0315	4.89	0.49
S_6	0.0747	5.62	S_6	0.0498	5.12	0.50
S_7	0.0175	5.89	S_8	0.0065	5.56	0.33
S_8	0.5895	6.05	S_7	0.4921	5.41	0.64
S_9	0.5518	6.12	S_{11}	0.2895	5.74	0.38

Water						
B3LYP			**DFT/MRCI**			**Correction**
State	**f**	**E_{vert}**	**State**	**f**	**E_{vert}**	**ΔE_{vert}**
S_1	0.0016	3.55	S_1	0.0156	3.67	-0.12
S_2	0.0701	3.94	S_2	0.0703	4.03	-0.09
S_3	0.0959	4.56	S_3	0.1208	4.48	0.08
S_4	0.0418	4.78	S_6	0.0427	5.07	-0.29
S_5	0.1525	4.81	S_4	0.1937	4.82	-0.01
S_6	0.1569	4.90	S_5	0.1980	4.84	0.06
S_7	0.0110	5.19	S_8	0.0061	5.49	-0.30
S_8	0.4668	5.50	S_7	0.4919	5.34	0.16
S_9	0.0370	5.54	S_9	0.0908	5.67	-0.13

Supporting Figures

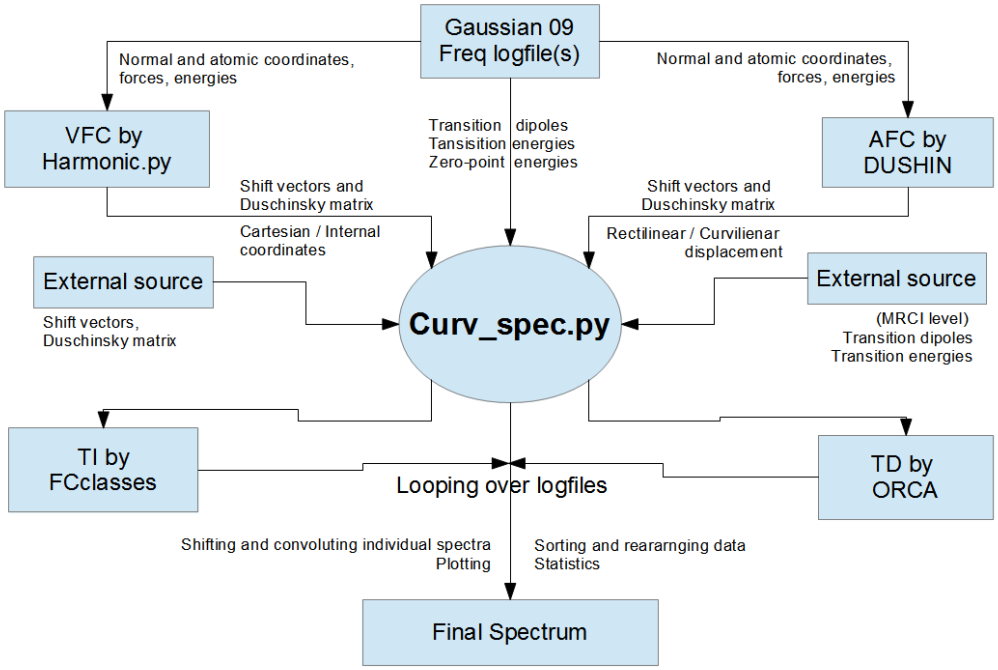

Figure S1. Workflow of the homemade script: Curv_spec.py

Software Capabilities:

-Generates vibrationally broadened TI and TD spectra using AFC and VFC schemes combined with IMDHO and IMDHO-FA (with and without Duschinsky rotation) models.

-Interface between Gaussian 09, DUSHIN, FCclasses, ORCA, and Harmonic.py.

-Compatible with G09 log files and formatted checkpoint files.

-Can work with more than one state and can convolute states.

-TI-FC and TD-FC formalisms as implemented in FCclasses and ORCA.

-AFC and VFC frameworks are implemented.

-Compatible with the use of Cartesian and internal coordinates.

-Reading external shift vectors and Duschinsky matrix to generate spectra.

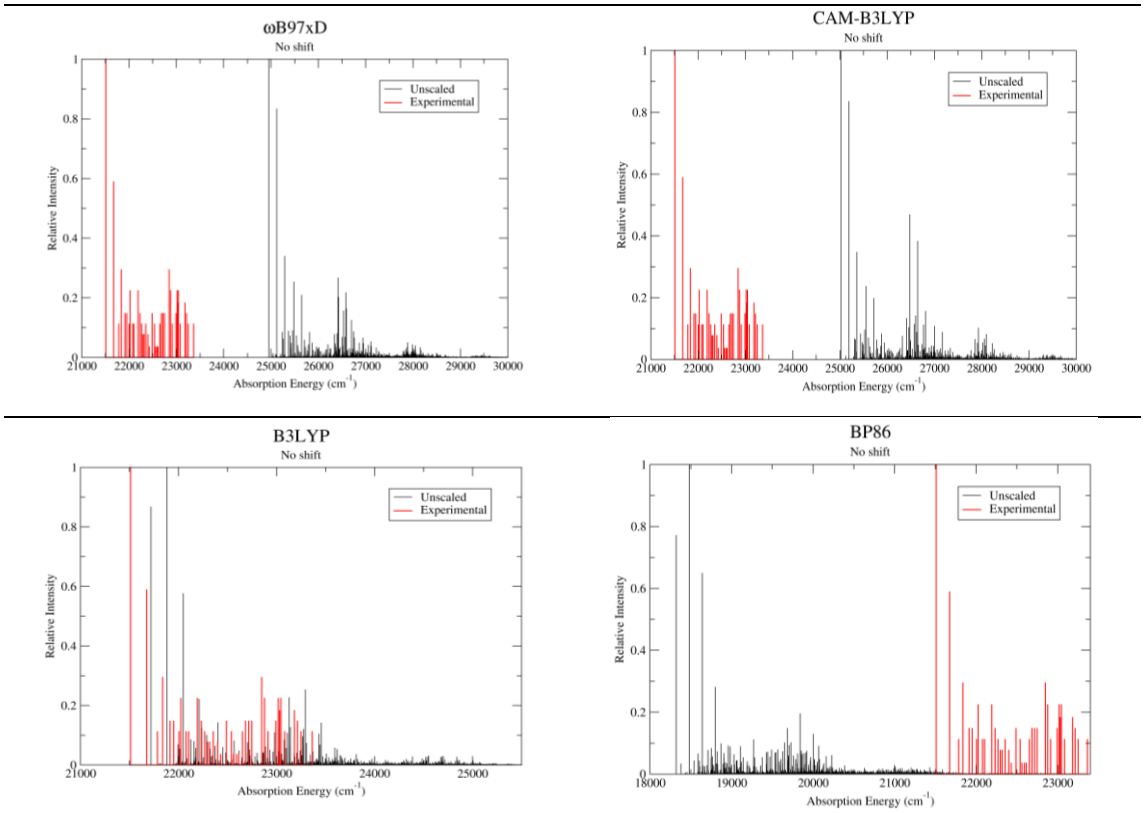

Figure S2. Comparison of the experimental absorption spectrum to original AFC stick spectra (see text for definition) for LF, S_1 state computed at the ωB97xD, CAM-B3LYP, B3LYP, and BP86 levels of theory with the 6-31G(d) basis-set using unscaled frequencies.

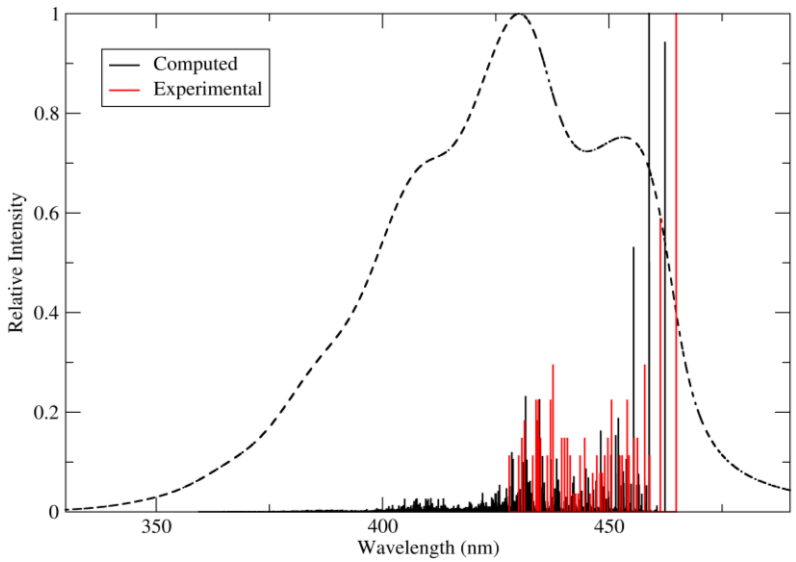

Figure S3. TI-AFC spectrum generated at the B3LYP/TZVP level using rectilinear coordinates in comparsion to the experiment. HWHM=250 cm^{-1} was used for broadening. At most 10^9 FC integrals were used. The convoluted theoretical spectrum is also shown (dashed line).

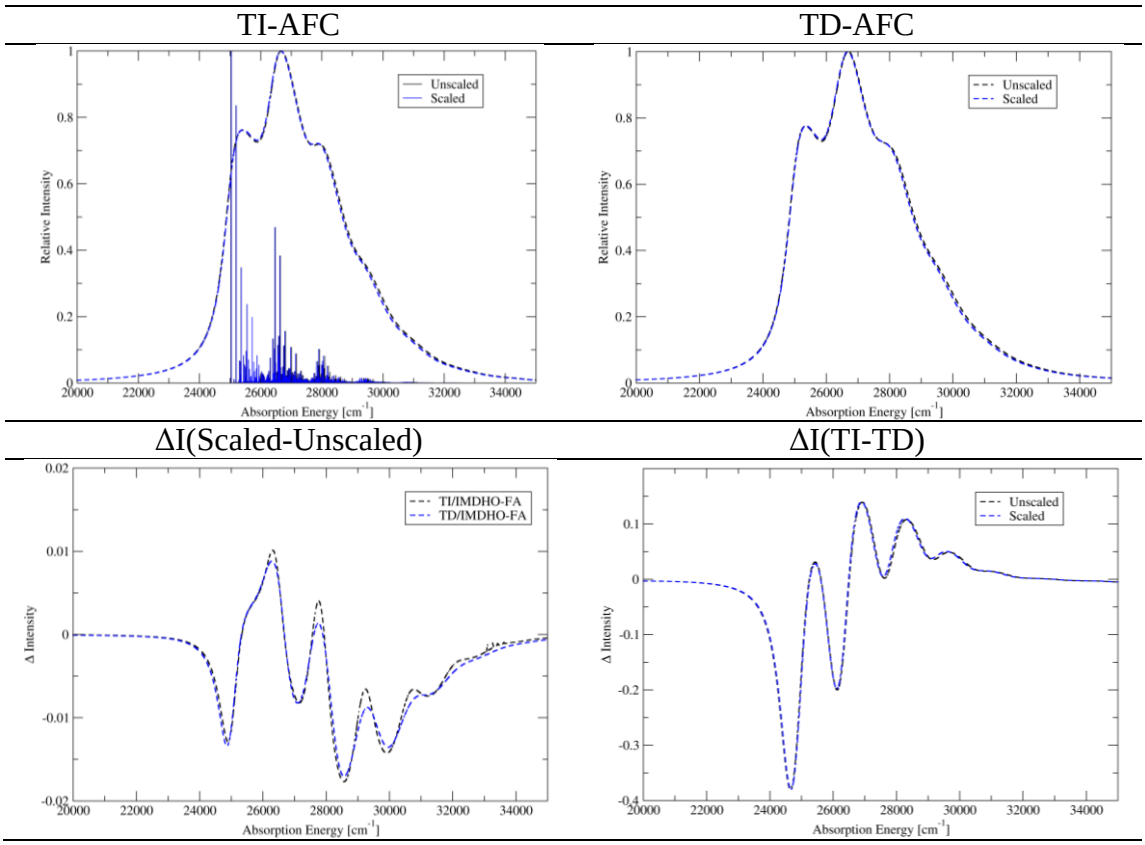

Figure S4. Top panel: TI-/TD-(IMDHO-FA)-AFC spectra of LF/S_1 at the eclipsed conformation computed at the CAM-B3LYP/6-31G(d) level using (black dashed line) unscaled and (blue dashed line) scaled frequencies. Bottom panel: Difference spectra of these methods. In TI spectrum, no Duschinsky rotation was applied for the sake of comparability. HWHM=403.275 cm^{-1} is used for broadening.

	0	10	20	30	40	50	60	70	80	90	100	110	120
S0	0.063	0.059	0.048	0.032	0.016	0.004	0	0.005	0.017	0.032	0.047	0.059	0.063
S1	0.052	0.049	0.04	0.027	0.013	0.003	0	0.004	0.014	0.027	0.04	0.049	0.052

Figure S5. CAM-B3LYP/6-31G(d) 1D scans of partially relaxed PES for LF/S_0 and LF/S_1 states in the gas phase along the dihedral angle (C8-C7-CMe-HMe) related to the C8-methyl torsion.

The other dihedral corresponding to the methyl group bound to C8 is kept fixed during constrained optimizations at the scan points. The calculations indicate an almost barrierless transformation between two conformations of LF (eclipsed and staggered) on both the S_0 and S_1 surfaces.

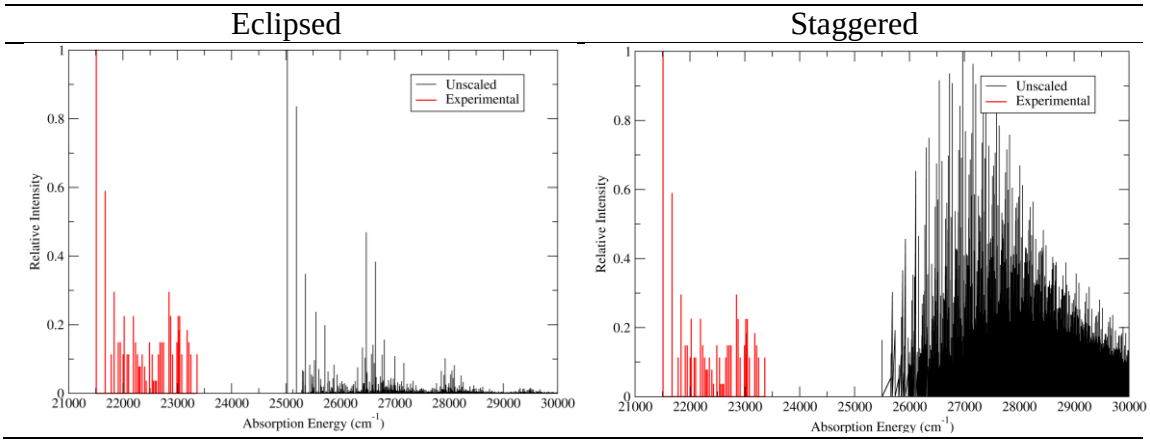

Figure S6. CAM-B3LYP/6-31G(d) TI-AFC stick spectra for two geometries with eclipsed and staggered conformations of LF/S_1 using the curvilinear representation.

At first sight, the spectrum for staggered conformation seems to have significantly more total intensity, which is however, not the case as is evident from the recovered fractions (Staggered: C=0.170 vs. eclipsed: C=0.947). The misleading impression comes from the chosen presentation (relative instead of absolute intensities).

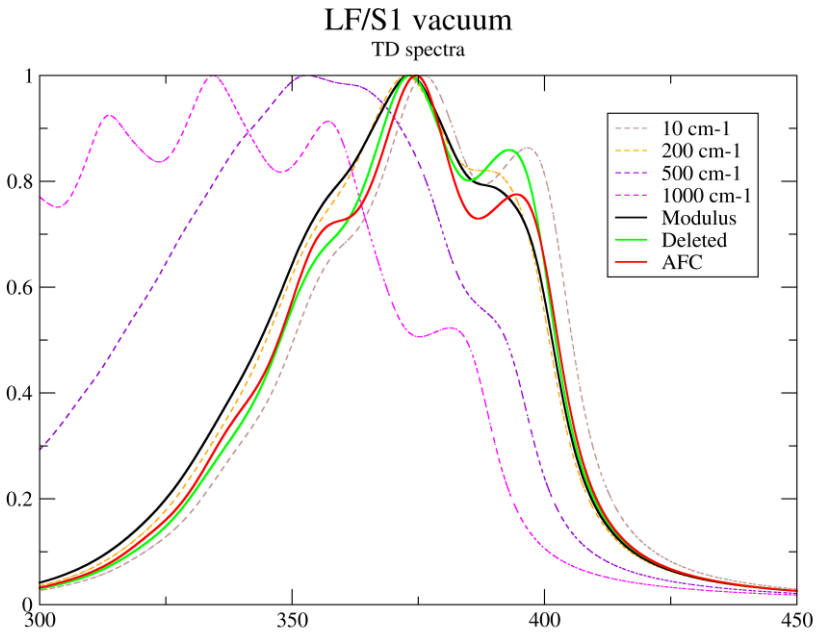

Figure S7. CAM-B3LYP level TD-VFC of LF/S_1 in which the imaginary frequency modes (i.e. 64 and 382*i* cm^{-1}) are deleted or replaced with an arbitrary positive number (10, 200, 500, 1000 cm^{-1}) or its modulus. The AFC spectrum is also given as a reference.

As evident from Figure S7, the deletion of the imaginary-frequency modes and related shift vector elements results in a spectrum with the highest similarity to the AFC spectrum that is taken as reference, given the availability of a real minimum geometry on the LF/S_1 energy surface. Replacing the modes with some arbitrary positive number (Figure S7, dashed lines) or its modulus (black solid line) can lead to

an unrealistic spectral topology. This can be explained by the high adimensional shift of an imaginary-frequency ES mode relative to its counterpart GS mode, which is caused by large unphysical gradients (due to being far away from a stationary point). By removing the contributions from imaginary-frequency modes, we can prevent introducing such unphysical effects in the computation of the broadened spectrum.

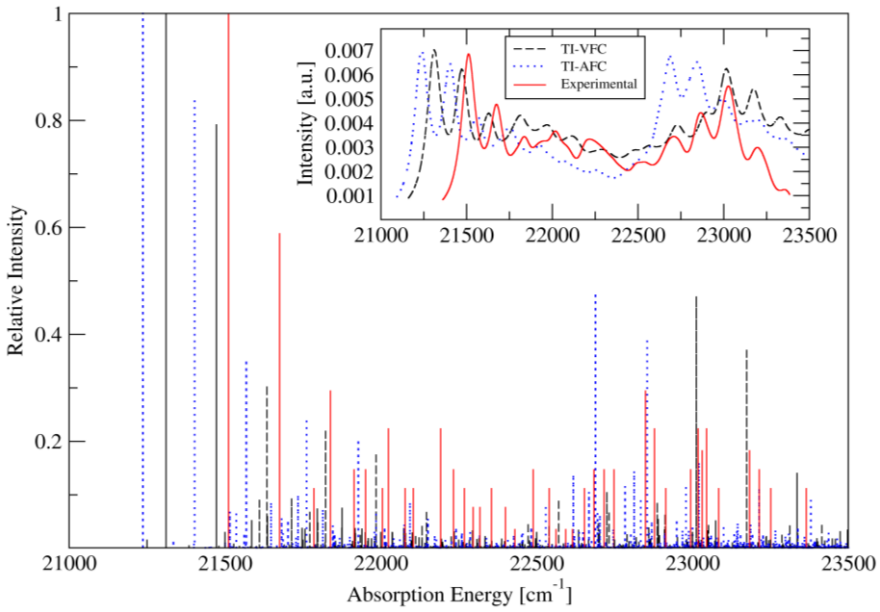

Figure S8. Comparison of MRCI-corrected TI-AFC and TI-VFC spectra of LF/S_1 in the gas phase computed at the CAM-B3LYP/6-31G(d) level to the experimental spectrum.

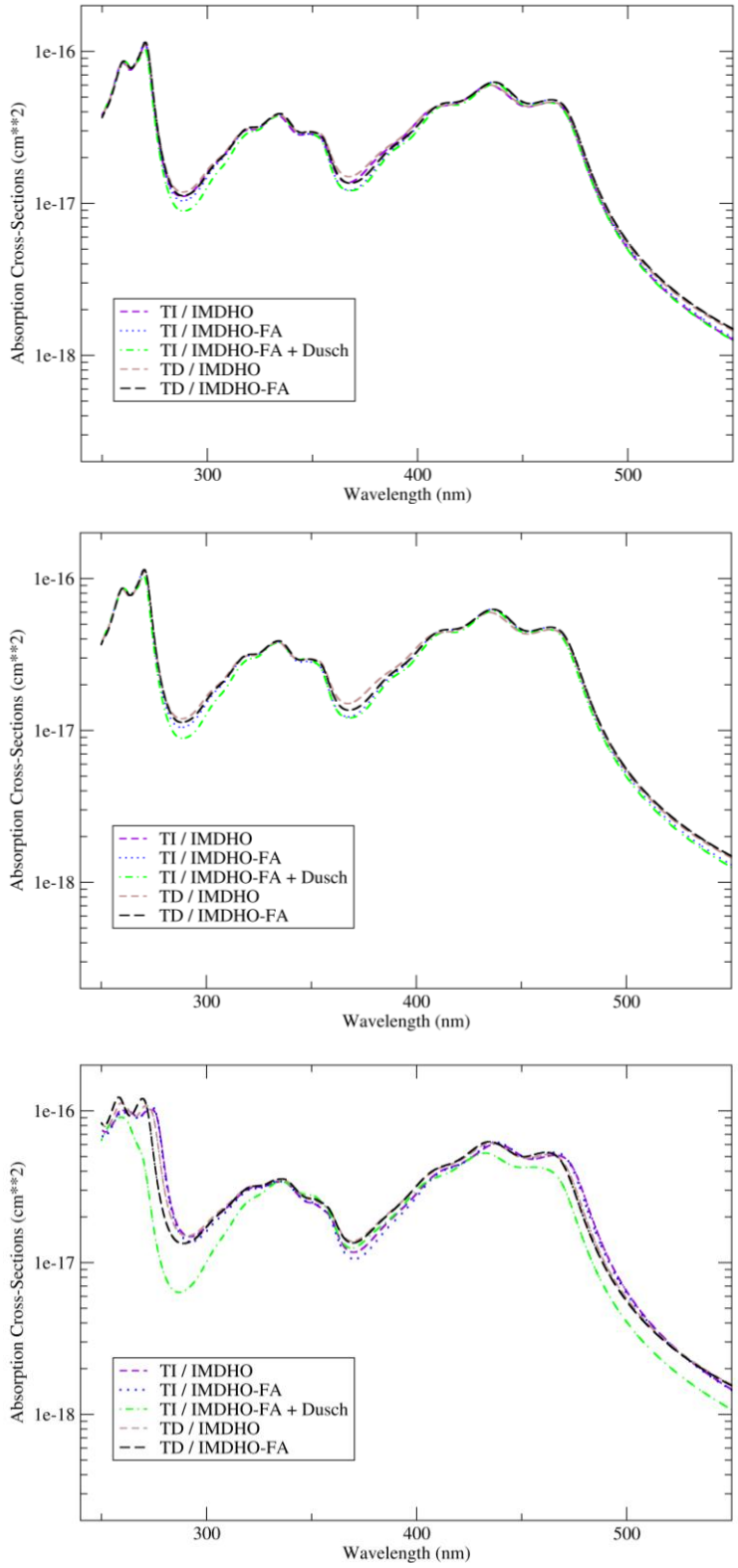

Figure S9. MRCI-corrected TI- and TD-FC spectra of LF in the gas phase computed at the CAM-B3LYP/6-31G(d) level. Top: AFC/rectilinear; middle: AFC/curvilinear; bottom: VFC.

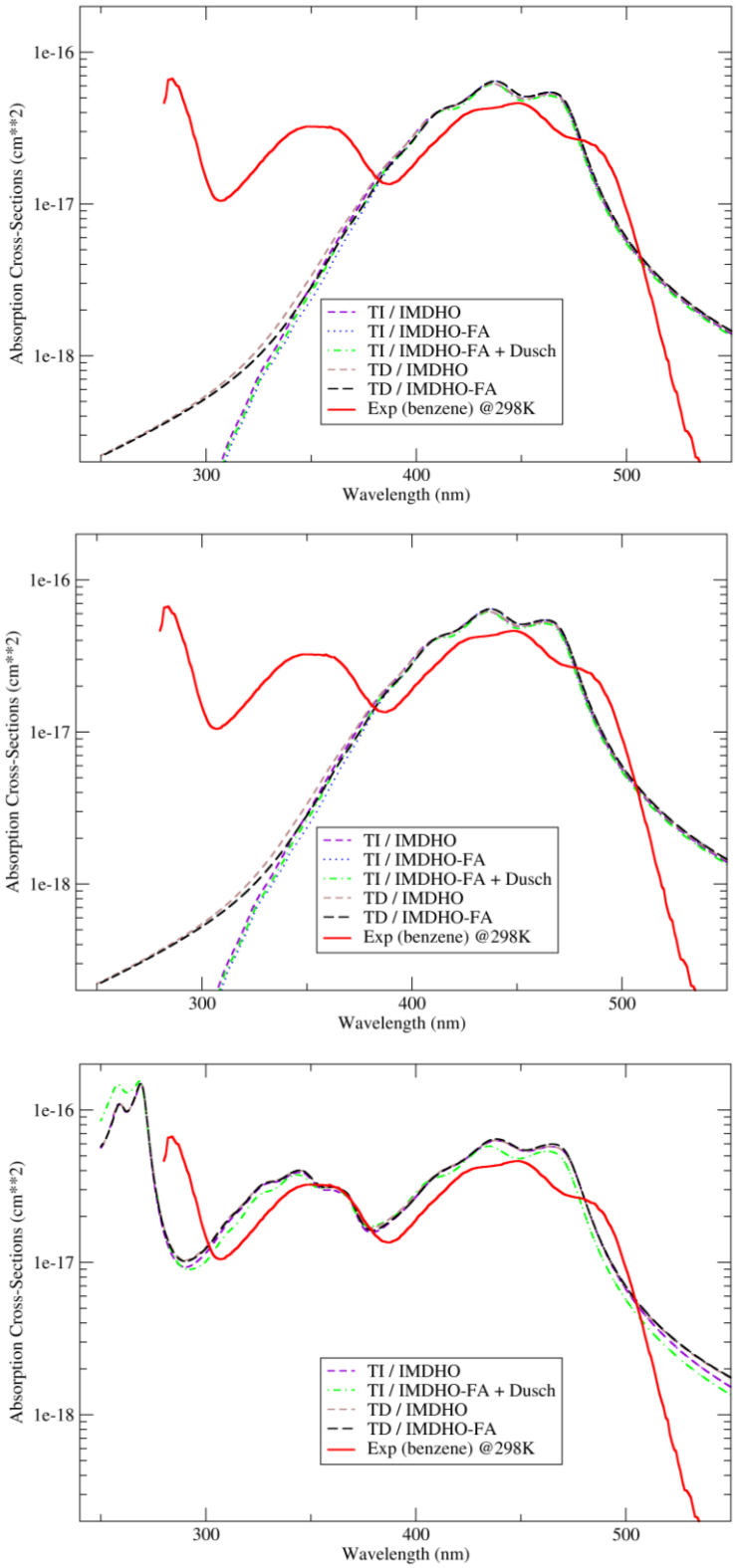

Figure S10. MRCI-corrected TI- and TD-FC spectra of LF in benzene computed at the CAM-B3LYP/6-31G(d) level. Top: AFC/rectilinear; middle: AFC/curvilinear; bottom: VFC.

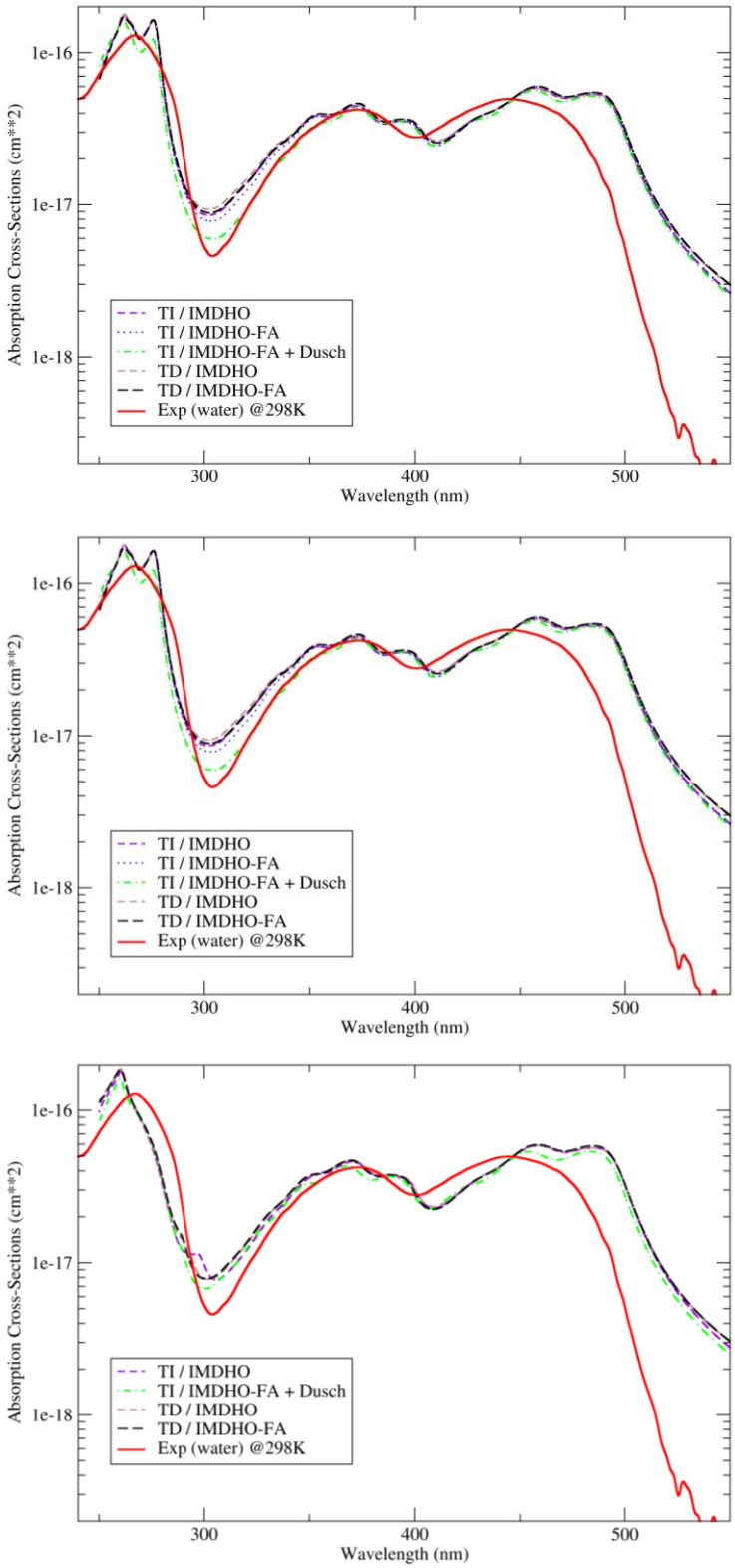

Figure S11. MRCI-corrected TI- and TD-FC spectra of LF in water computed at the CAM-B3LYP/6-31G(d) level. Top: AFC/rectilinear; middle: AFC/curvilinear; bottom: VFC.

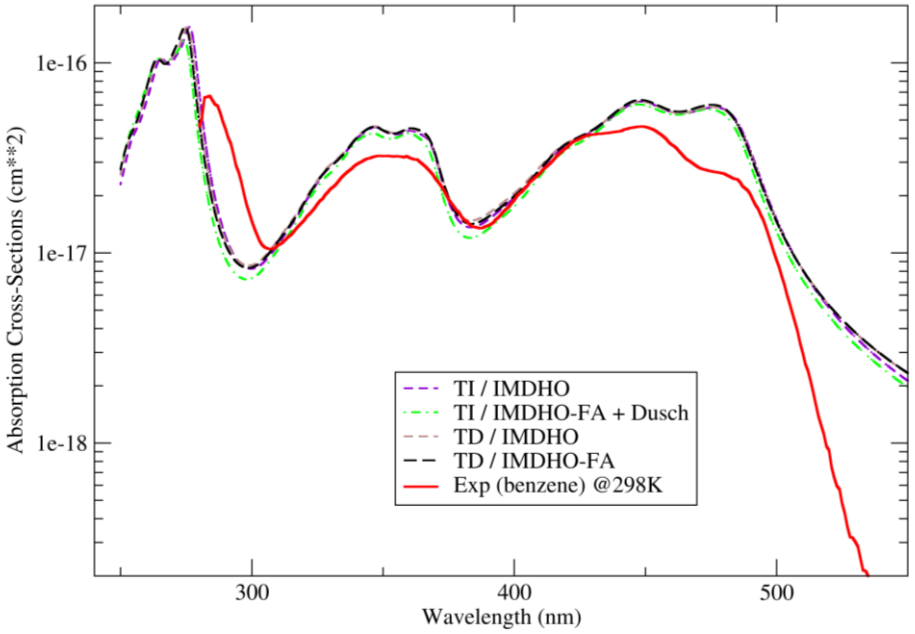

Figure S12. MRCI-corrected TI- and TD-VFC spectra of LF in benzene computed at the B3LYP/6-31G(d) level.

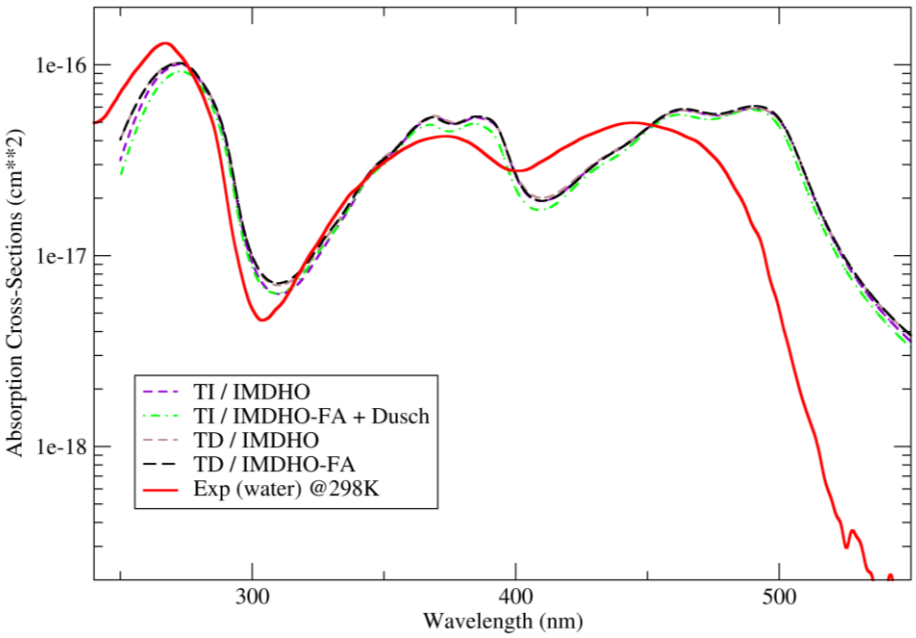

Figure S13. MRCI-corrected TI- and TD-VFC spectra of LF in water computed at the B3LYP/6-31G(d) level.

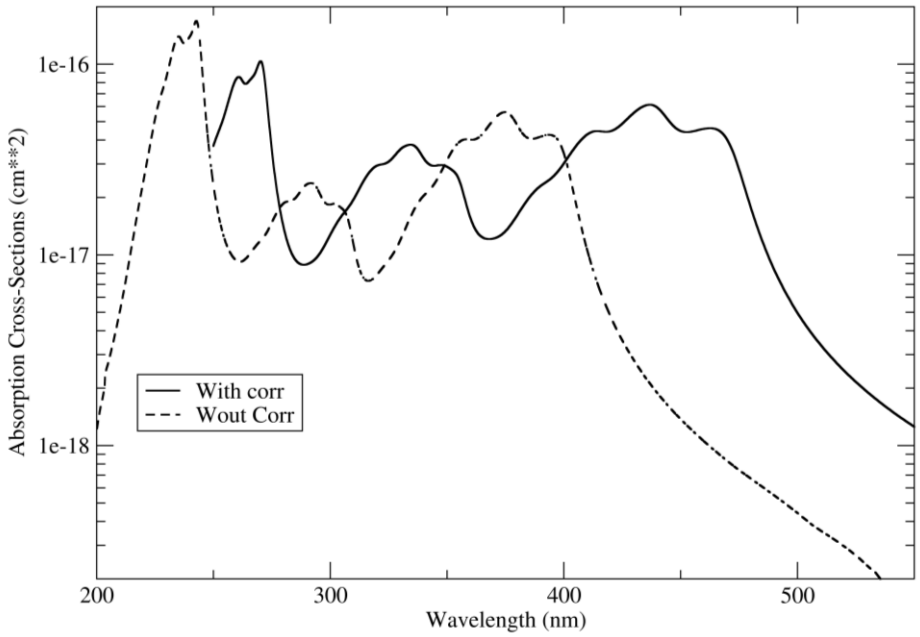

Figure S14. Comparison of TI/IMDHO-FA (with Duschinsky mixing) VFC spectra of LF in the gas phase at the CAM-B3LYP/6-31G(d) level with (solid line) and without (dashed line) MRCI correction for the 0-0 peak positions and relative intensities of each electronically excited state (see main text for details).

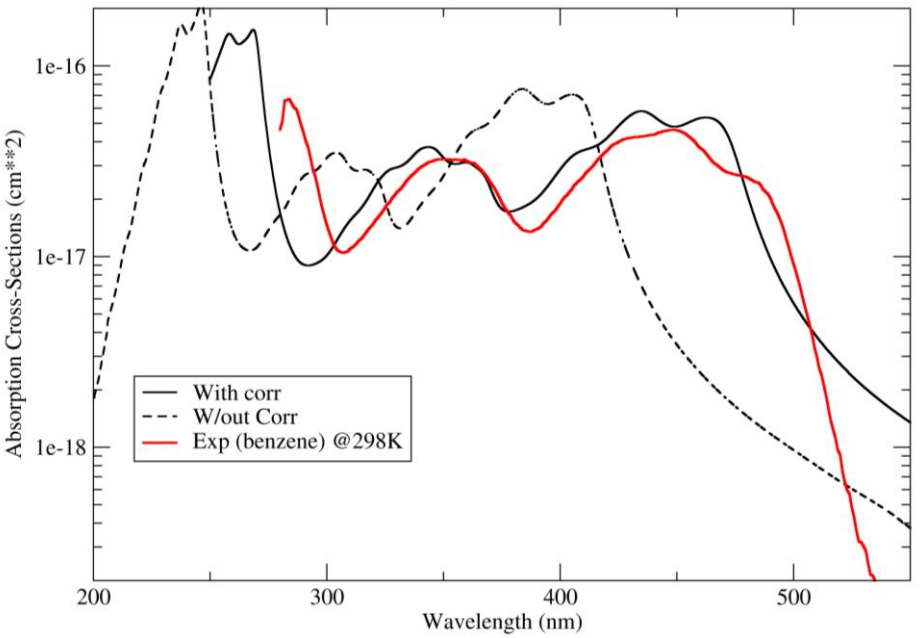

Figure S15. Comparison of TI/IMDHO-FA (with Duschinsky mixing) VFC spectra of LF in benzene at the CAM-B3LYP/6-31G(d) level with (solid line) and without

(dashed line) MRCI correction for the 0-0 peak positions and relative intensities of each electronically excited state (see text for details). The experimental spectrum (from ref [8]) is also given.

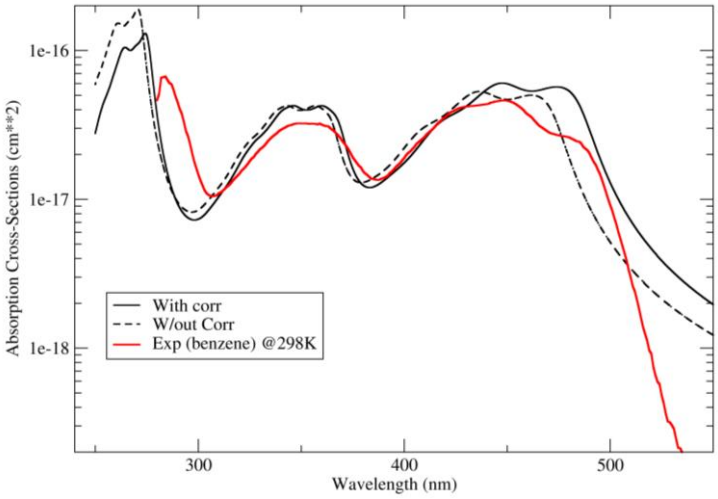

Figure S16. Comparison of TI/IMDHO-FA (with Duschinsky mixing) VFC spectra of LF in benzene at the B3LYP/6-31G(d) level with (solid line) and without (dashed line) MRCI correction for the 0-0 peak positions and relative intensities of each electronically excited state (see main text for details). The experimental spectrum (from ref [8]) is also given.

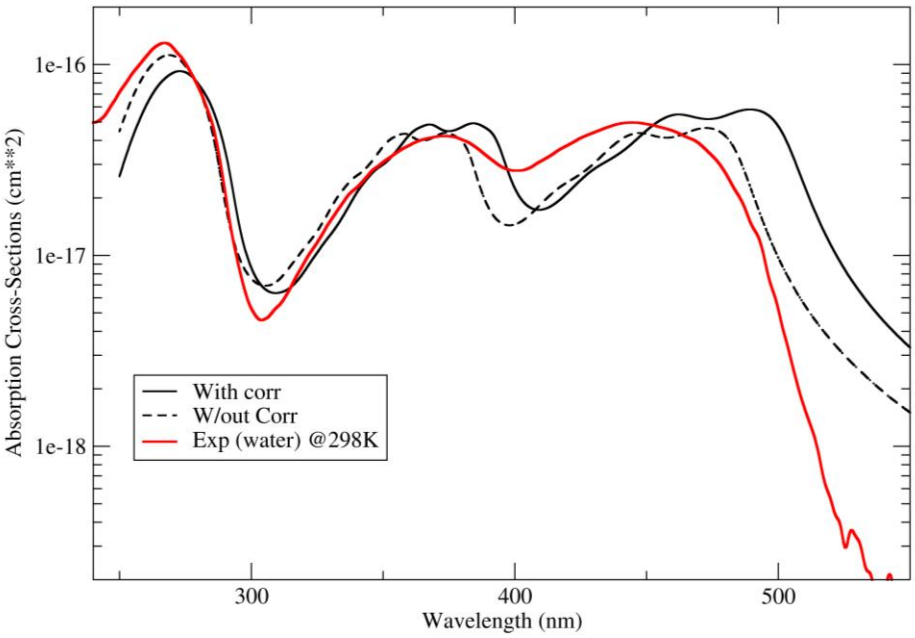

Figure S17. Comparison of TI/IMDHO-FA (with Duschinsky mixing) VFC spectra of LF in water at the B3LYP/6-31G(d) level with (solid line) and without (dashed line) MRCI correction for the 0-0 peak positions and relative intensities of each electronically excited state (see main text for details). The experimental spectrum (from ref [8]) is also given.

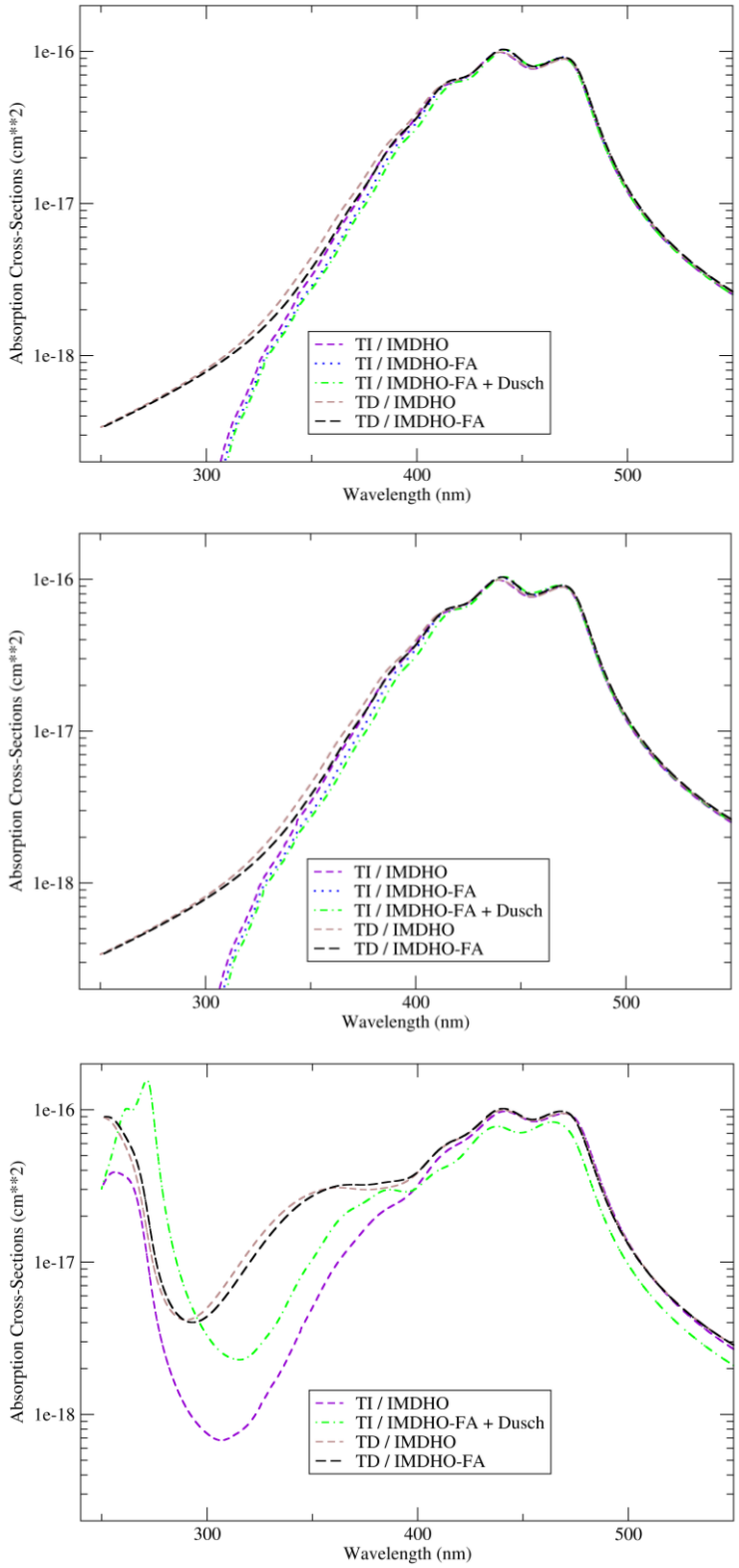

Figure S18. MRCI-corrected TI- and TD-FC spectra of RoLF in the gas phase computed at the CAM-B3LYP/6-31G(d) level. Top: AFC/rectilinear; middle: AFC/curvilinear; bottom: VFC.

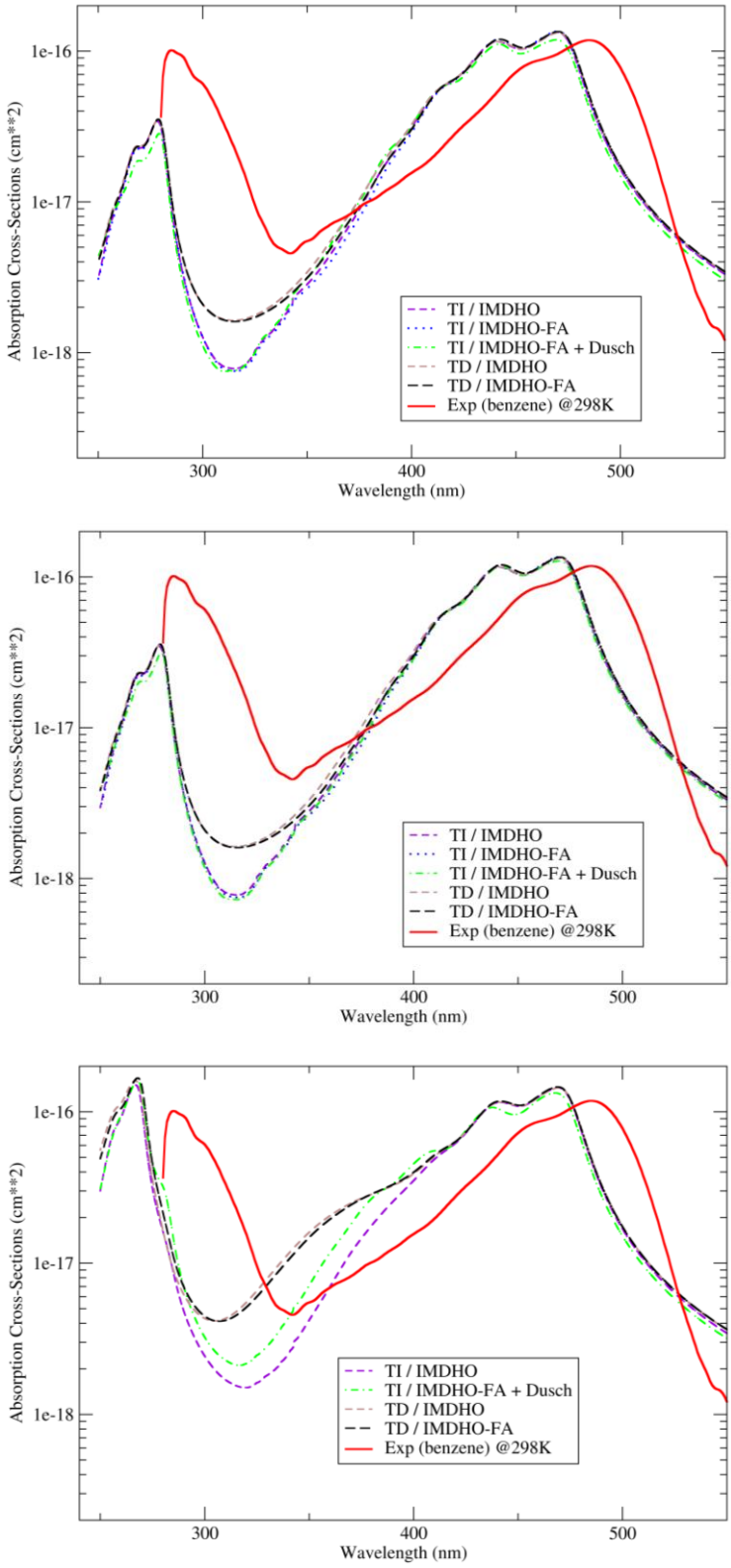

Figure S19. MRCI-corrected TI- and TD-FC spectra of RoLF in benzene computed at the CAM-B3LYP/6-31G(d) level. Top: AFC/rectilinear; middle: AFC/curvilinear; bottom: VFC.

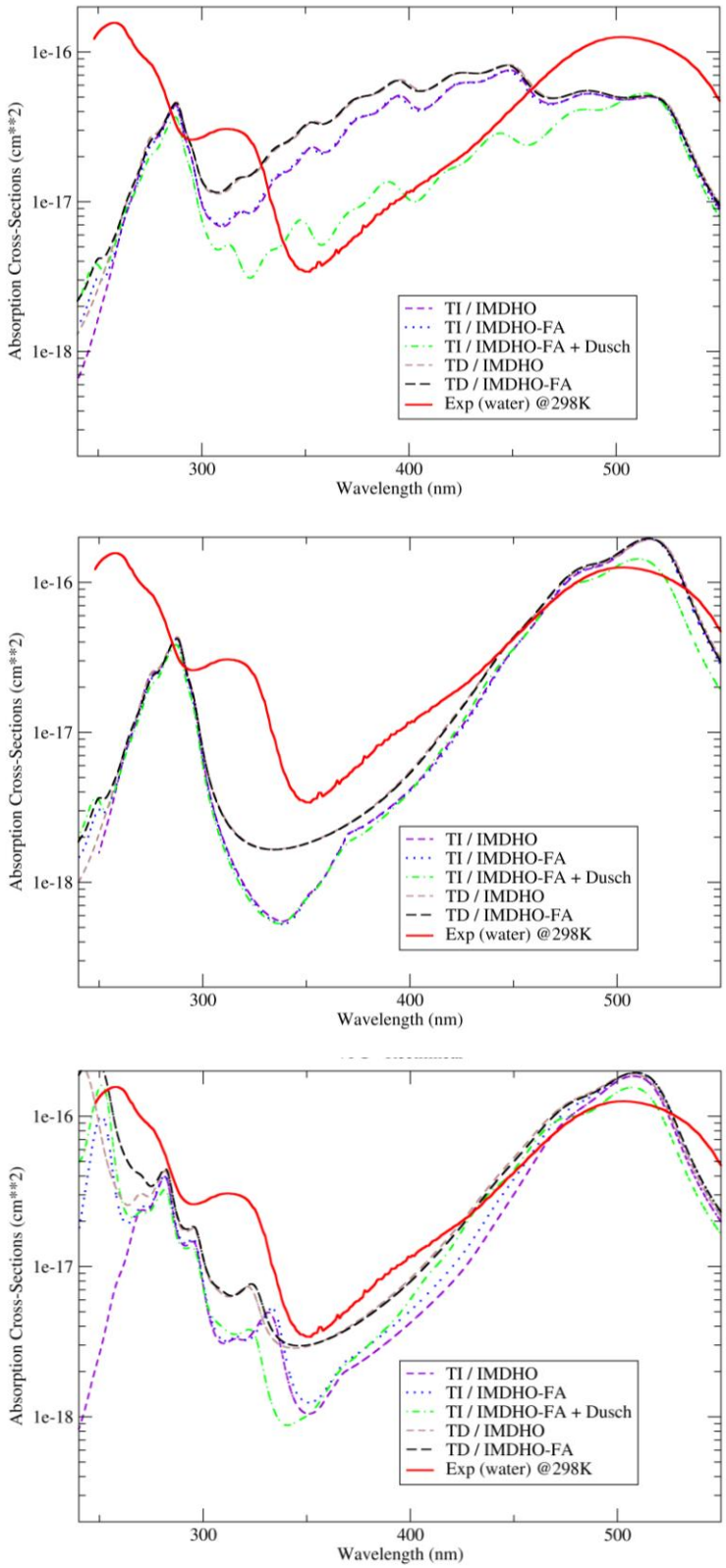

Figure S20. MRCI-corrected TI- and TD-FC spectra of RoLF in water computed at the CAM-B3LYP/6-31G(d) level. Top: AFC/rectilinear; middle: AFC/curvilinear; bottom: VFC.

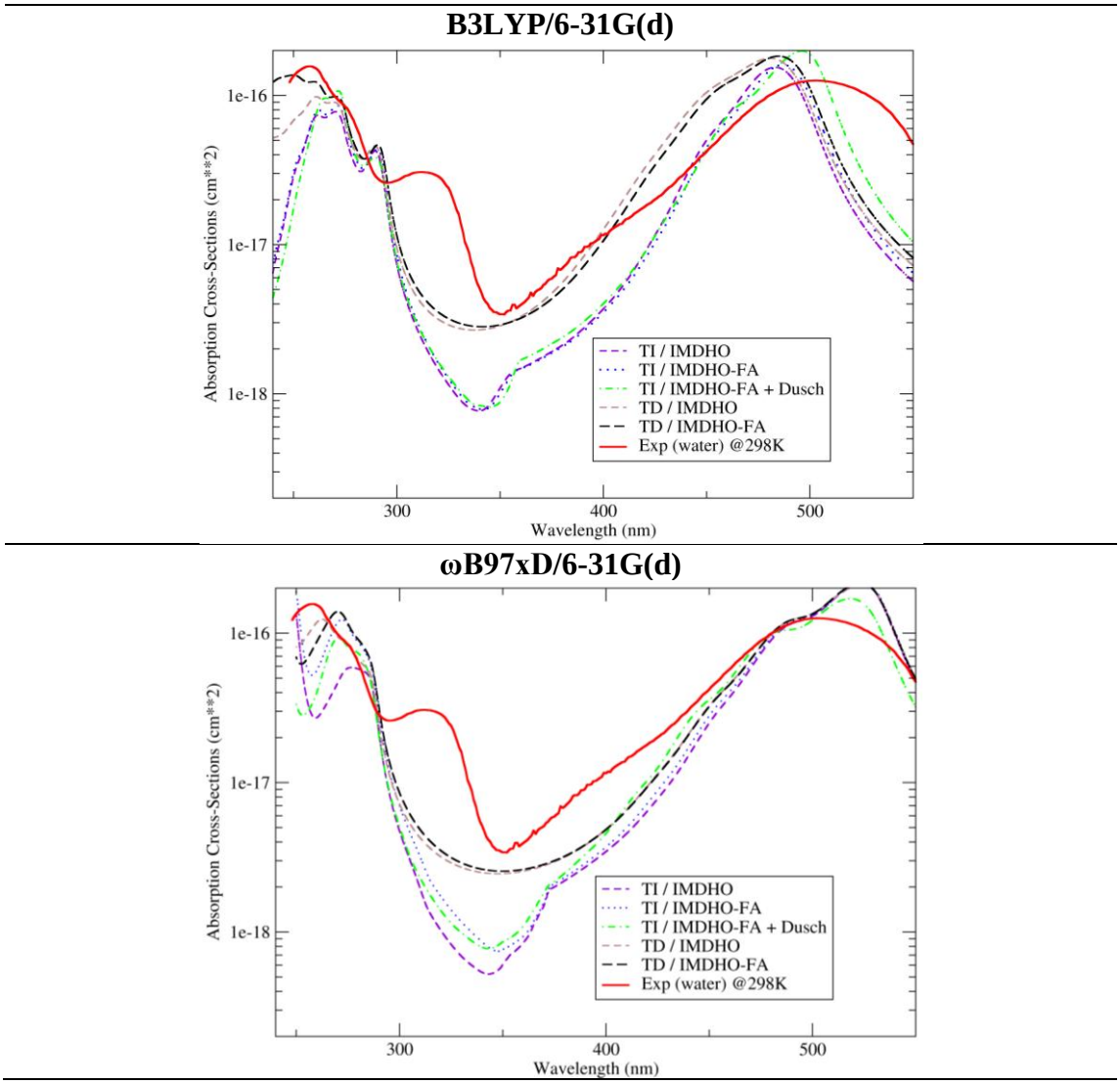

Figure S21. MRCI-corrected convoluted (TI-/TD-)VFC spectra of **RoLF** computed at 0.01K **in water** in comparison to the experimentally measured spectrum at 298K (taken from ref [8]). B3LYP and ωB97xD spectra are compared.

Comparing VFC spectra from different functionals (Figure S20, bottom panel and Figure S21) further, we notice that the spectra from ωB97xD agree well with those from CAM-B3LYP for the first band, albeit with a minute red shift. The spectra from B3LYP, conversely, differ to a visible degree in terms of shape and blue-shifted band position. The latter point appears to be originating from (a) dissimilar GS minima: the B3LYP geometry deviates from the CAM-B3LYP geometry substantially (RMSD: 0.029Å) as compared to the ωB97xD (RMSD: 0.014Å), and (b) different Hessians

with concomitant deviations in the reorganization energies: λ_{ES} at the B3LYP, CAM-B3LYP, and ωB97xD levels amounts to 0.11 eV, 0.16 eV, and 0.17 eV, respectively, pointing again to the similarity of CAM-B3LYP and ωB97xD. Finally, for the third band each functional gives a different picture, with B3LYP apparently best matching experiment.

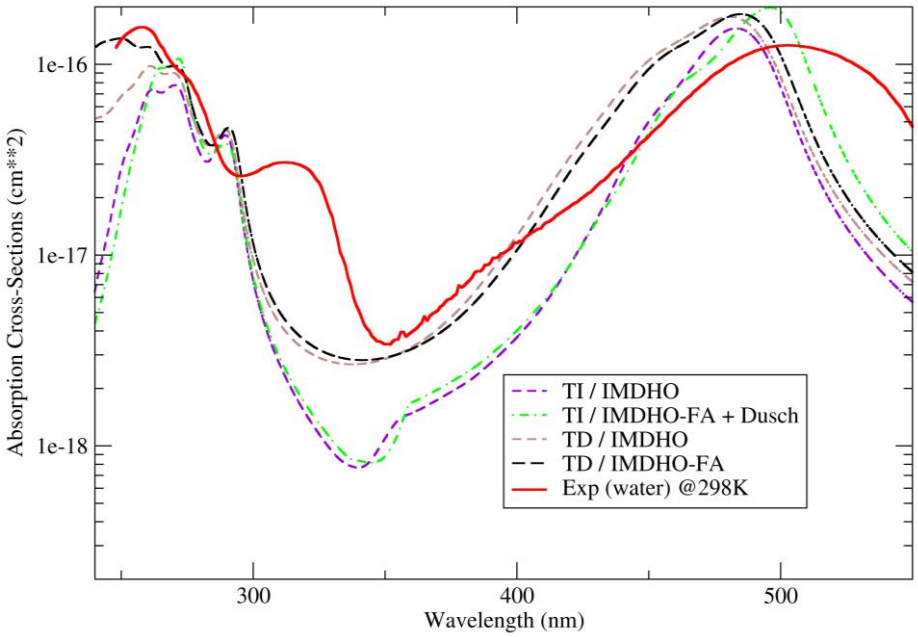

Figure S22. Original TI- and TD-VFC spectra of RoLF in water computed at the B3LYP/6-31G(d) level (i.e. without MRCI-correction).

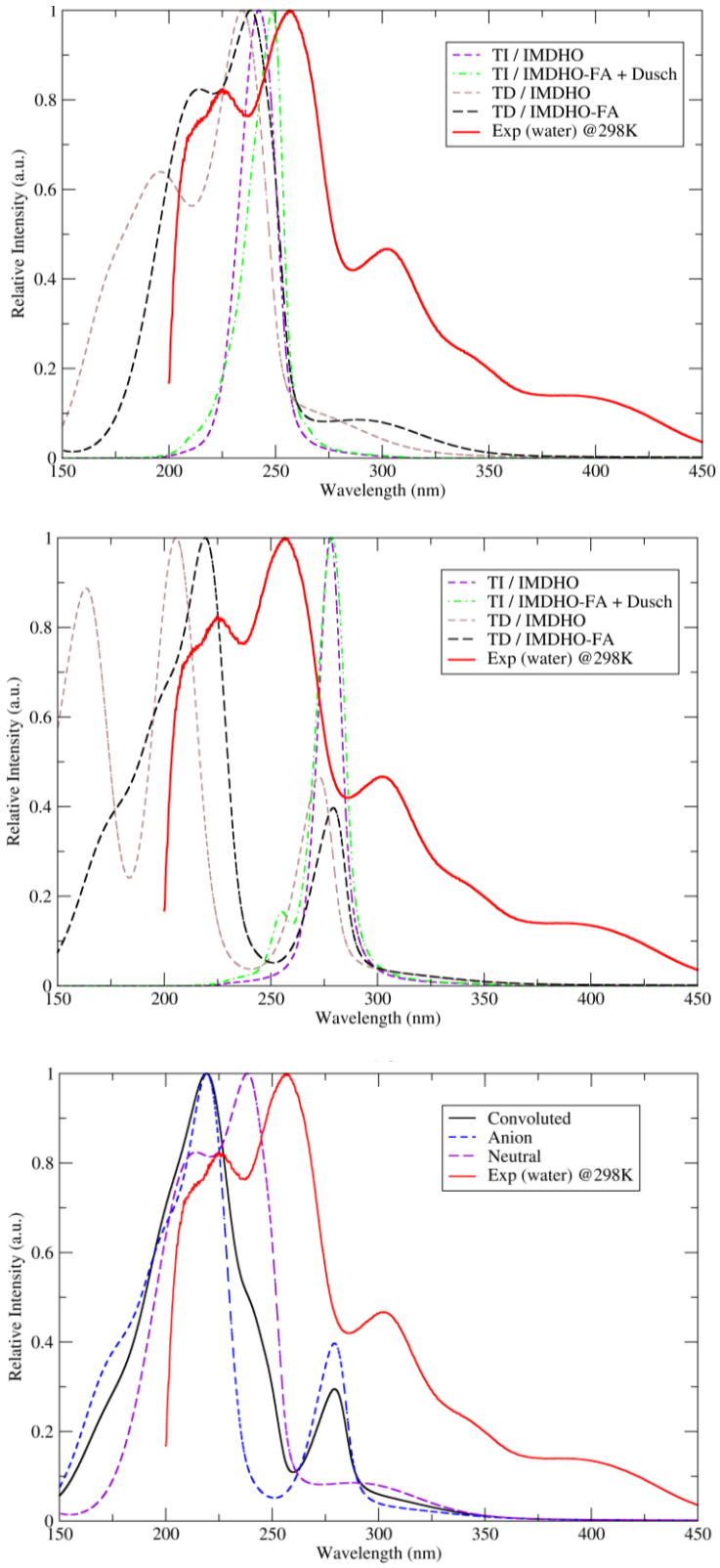

Figure S23. MRCI-corrected CAM-B3LYP/6-31G(d) level TI and TD VFC spectra of neutral (top), anionic (middle) form of 5TLF in water and the combination of the TD/IMDHO-FA of both forms (bottom).

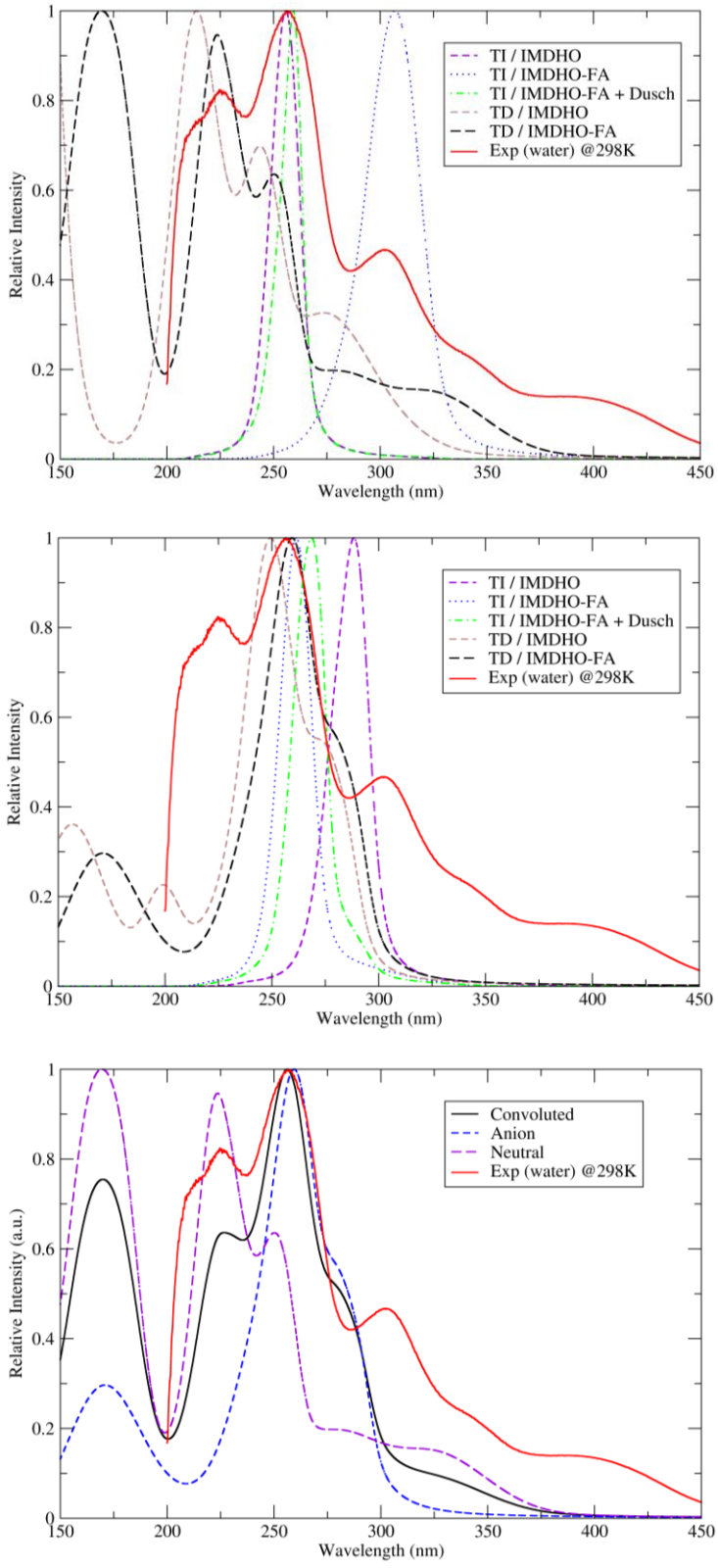

Figure S24. MRCI-corrected B3LYP/6-31G(d) level TI and TD VFC spectra of neutral (top), anionic (middle) form of 5TLF in water and the combination of the TD/IMDHO-FA of both forms (bottom).

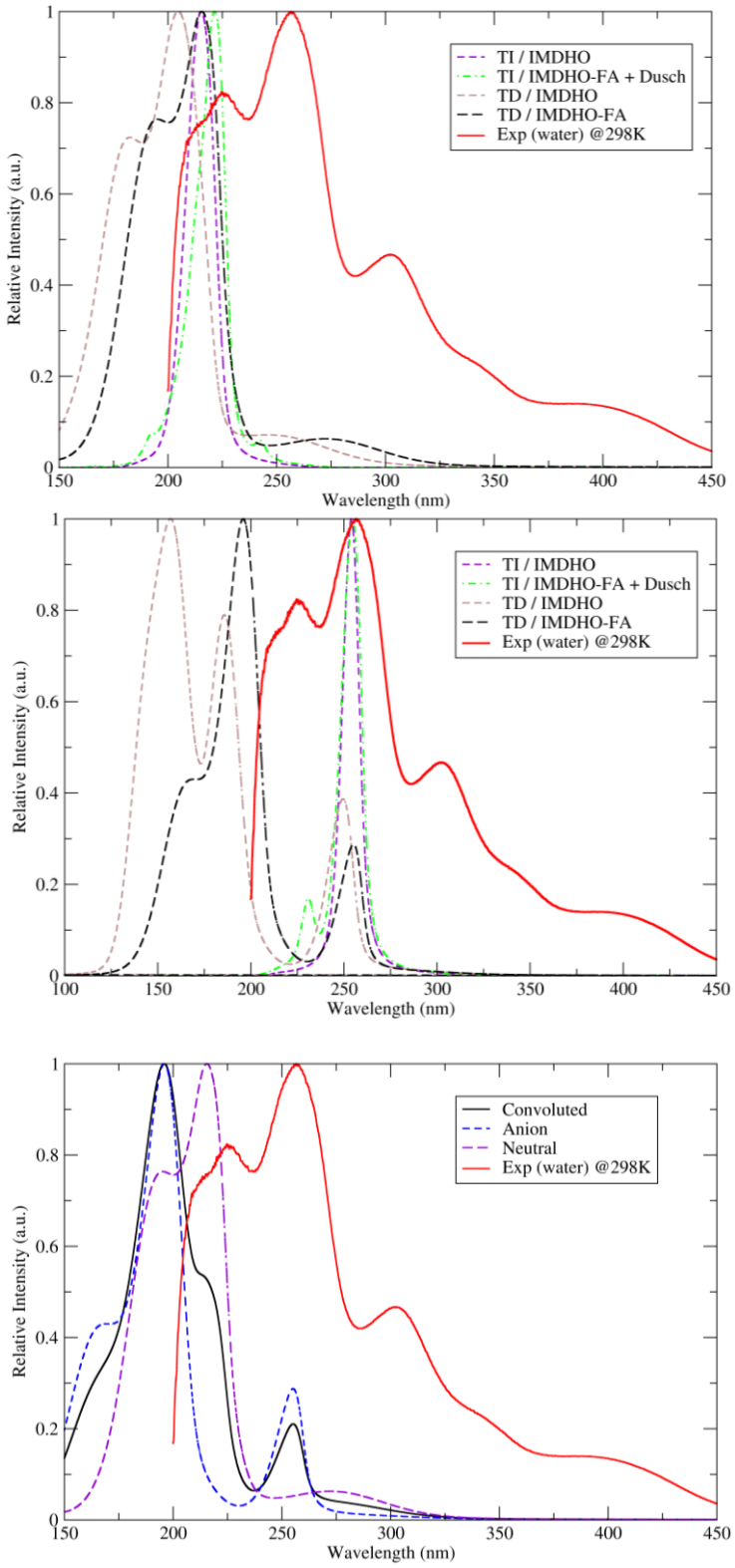

Figure S25. CAM-B3LYP/6-31G(d) TI and TD VFC spectra of the neutral (top) and anionic (middle) form of 5TLF in water; TD/IMDHO-FA spectra of 1:1 mixture of both forms (bottom). No MRCI correction was applied, original spectra are presented.

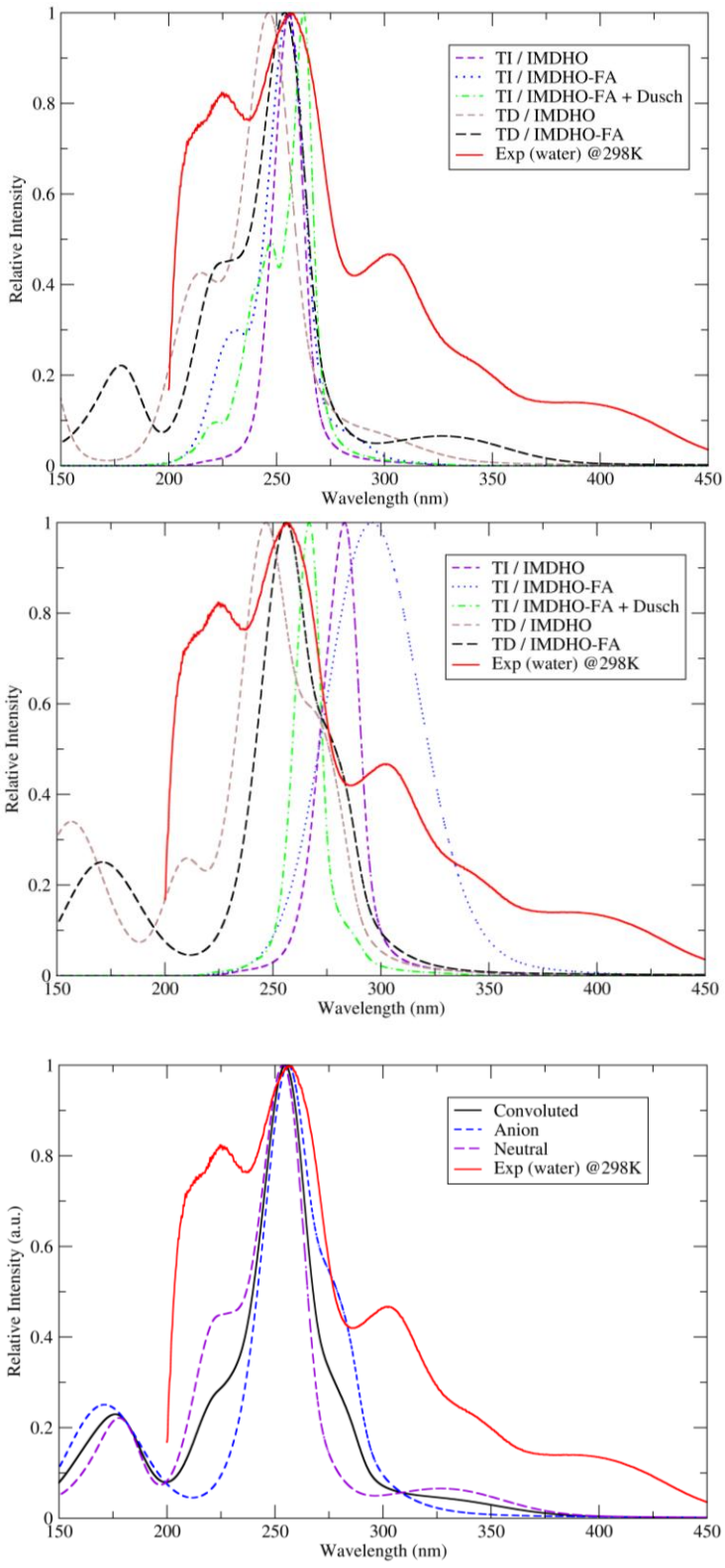

Figure S26. B3LYP/6-31G(d) level TI and TD VFC spectra of neutral (top) and anionic (middle) form of 5TLF in water; TD/IMDHO-FA spectra of 1:1 mixture of both forms (bottom). No MRCI correction was applied, original spectra are presented.

REFERENCES

(1) Niu, Y.; Peng, Q.; Deng, C.; Gao, X.; Shuai, Z. Theory of Excited State Decays and Optical Spectra: Application to Polyatomic Molecules. *J. Phys. Chem. A* **2010**, *114*, 7817–7831.

(2) Saven, J. G.; Skinner, J. L. A Molecular Theory of the Line Shape: Inhomogeneous and Homogeneous Electronic Spectra of Dilute Chromophores in Nonpolar Fluids. *J. Chem. Phys.* **1993**, *99*, 4391.

(3) Crespo-Otero, R.; Barbatti, M. Spectrum Simulation and Decomposition with Nuclear Ensemble: Formal Derivation and Application to Benzene, Furan and 2-Phenylfuran. *Theor. Chem. Acc.* **2012**, *131*, 1237.

(4) Alecu, I. M.; Zheng, J.; Zhao, Y.; Truhlar, D. G. Computational Thermochemistry: Scale Factor Databases and Scale Factors for Vibrational Frequencies Obtained from Electronic Model Chemistries - SI. *J. Chem. Theory Comput.* **2010**, *6*, 1–10.

(5) Vdovin, A.; Slenczka, A.; Dick, B. Electronic Spectroscopy of Lumiflavin in Superfluid Helium Nanodroplets. *Chem. Phys.* **2013**, *422*, 195–203.

(6) Salzmann, S.; Tatchen, J.; Marian, C. M. The Photophysics of Flavins: What Makes the Difference between Gas Phase and Aqueous Solution? *J. Photochem. Photobiol. A Chem.* **2008**, *198*, 221–231.

(7) Salzmann, S.; Martinez-Junza, V.; Zorn, B.; Braslavsky, S. E.; Mansurova, M.; Marian, C. M.; Gärtner, W. Photophysical Properties of Structurally and Electronically Modified Flavin Derivatives Determined by Spectroscopy and Theoretical Calculations. *J. Phys. Chem. A* **2009**, *113*, 9365–9375.

(8) Zirak, P.; Penzkofer, A.; Mathes, T.; Hegemann, P. Photo-Dynamics of Roseoflavin and Riboflavin in Aqueous and Organic Solvents. *Chem. Phys.* **2009**, *358*, 111–122.